

CANADIAN THESES ON MICROFICHE

THÈSES CANADIENNES SUR MICROFICHE



National Library of Canada
Collections Development Branch

Canadian Theses on
Microfiche Service

Ottawa, Canada
K1A 0N4

Bibliothèque nationale du Canada
Direction du développement des collections

Service des thèses canadiennes
sur microfiche

NOTICE

The quality of this microfiche is heavily dependent upon the quality of the original thesis submitted for microfilming. Every effort has been made to ensure the highest quality of reproduction possible.

If pages are missing, contact the university which granted the degree.

Some pages may have indistinct print especially if the original pages were typed with a poor typewriter ribbon or if the university sent us an inferior photocopy.

Previously copyrighted materials (journal articles, published tests, etc.) are not filmed.

Reproduction in full or in part of this film is governed by the Canadian Copyright Act, R.S.C. 1970, c. C-30. Please read the authorization forms which accompany this thesis.

**THIS DISSERTATION
HAS BEEN MICROFILMED
EXACTLY AS RECEIVED**

AVIS

La qualité de cette microfiche dépend grandement de la qualité de la thèse soumise au microfilmage. Nous avons tout fait pour assurer une qualité supérieure de reproduction.

S'il manque des pages, veuillez communiquer avec l'université qui a conféré le grade.

La qualité d'impression de certaines pages peut laisser à désirer, surtout si les pages originales ont été dactylographiées à l'aide d'un ruban usé ou si l'université nous a fait parvenir une photocopie de qualité inférieure.

Les documents qui font déjà l'objet d'un droit d'auteur (articles de revue, examens publiés, etc.) ne sont pas microfilmés.

La reproduction, même partielle, de ce microfilm est soumise à la Loi canadienne sur le droit d'auteur, SRC 1970, c. C-30. Veuillez prendre connaissance des formules d'autorisation qui accompagnent cette thèse.

**LA THÈSE A ÉTÉ
MICROFILMÉE TELLE QUE
NOUS L'AVONS REÇUE**

Canada

INTENSITY DEPENDENT PHOTOCONDUCTIVITY AND PHOTOLUMINESCENCE IN CdIn_2S_4

by

Sylvain Charbonneau

Thesis submitted to the School of Graduate Studies
in partial fulfilment of the requirements for
the degree of Master of Science in Physics

Department of Physics

Faculty of Science and Engineering

University of Ottawa

Ottawa, Canada

1985

© Sylvain Charbonneau, Ottawa, Canada, 1985.

ABSTRACT

Photoconductivity spectra of CdIn_2S_4 at 300 K and 100 K, in the 1.7 eV to 3.0 eV excitation range, were used for the determination of the energies of the transitions involving the impurity levels in our samples. The photocurrent, which is proportional to the number of free carriers produced by the exciting light, was then measured for intrinsic and some specific extrinsic transitions as a function of light intensity over a maximum of twelve orders of magnitude (10^{16} to 10^{28} photons/m²-sec). For certain wavelength ranges, a photoconductivity plateau was observed at high excitation light intensities. This effect was attributed to a saturation of the high density levels within the gap at high light intensities. In comparison, sublinear behaviour was observed for some other wavelengths in the photoconductivity versus intensity experiment.

Photoconductivity (PC) transient experiments were performed in order to determine the variation of the rise and decay times of the PC signals as a function of excitation intensity at two different temperatures. These experiments provided information necessary for the complete analysis of the PC spectra obtained through laser excitation. Some optical absorption versus intensity experiments were also done in order to determine whether the saturation effect observed with the PC technique could also be seen by optical absorption.

Finally, photoluminescence spectra were recorded between 4.2 K and 300 K in order to investigate the radiative recombination processes.

only one type of process by which free carriers decay. The luminescence spectra were useful in the characterization of the samples. Some preliminary results on the variation of luminescence intensity and photoluminescence transient with exciting light intensity were investigated at some specific wavelengths in the hope of detecting superradiance.

ACKNOWLEDGMENTS

I would like, first of all, to thank Dr. E. Fortin for his suggestion of the thesis topic and for his advice during the course of the project. I am also very appreciative of the innumerable occasions on which I have been aided by the staff and students of the Physics department. A special thanks is due to D. Crandles and E. Tselepis for their helpful suggestions and to Dr. A. Anedda who did some of the pioneer work and who provided the samples for this work.

I am very grateful to the Natural Science and Engineering Research Council of Canada for their financial assistance.

Finally, I wish to express my sincere gratitude to my parents for their encouragement and for providing an atmosphere conducive to achievement.

TABLE OF CONTENTS

ABSTRACT 1

ACKNOWLEDGMENTS iii

LIST OF FIGURES vi

LIST OF TABLES vii

ABBREVIATIONS viii

CHAPTER I INTRODUCTION

I.1 Origins of the project 1

I.2 Summary of the project 4

I.3 Scheme of the project 6

CHAPTER II THEORY

II.1 General description of PC phenomena 9

II.2 Theoretical model for linear and sublinear
behaviour of PC versus intensity 19

II.3 Photoluminescence 25

II.4 Energy band diagrams of CdIn₂S₄ 26

CHAPTER III EXPERIMENTAL TECHNIQUES

III.1	Sample preparation	29
III.2	Relevance of good ohmic contact	30
III.3	Photoconductivity experiment	32
III.4	Laser CMX-4 description	37
III.5	Photoluminescence experiment	39

CHAPTER IV RESULTS AND DISCUSSION

IV.1	Photoluminescence spectra	41
IV.2	Photoconductivity spectra	45
IV.3	PC versus intensity (low light intensity)	48
IV.4	PC versus intensity and PC transient kinetics (high light intensity)	51
IV.5	Intensity dependent absorption	63
IV.6	PL versus intensity and PL transient kinetics	66

CHAPTER V SUMMARY AND CONCLUSION

75

APPENDIX A.	78
APPENDIX B.	80
REFERENCES	81

LIST OF FIGURES

- 1.1 A quarter of the fcc spinel unit cell
- 2.1 Model for exponents of current-light curve lying between 0.5 and 1.0
a) Unilluminated; b) Illuminated
- 2.2 Energy-level scheme and model of recombination processes of photo-excited carriers in CdIn_2S_4 at LNT
- 3.1 Representation of a neutral contact
a) volume unilluminated; b) volume illuminated
- 3.2 I-V characteristics at RT and 100 K in the dark (Sample 1)
- 3.3 a) sample holder ; b) measuring circuit for PC experiment
- 3.4 Experimental apparatus for the high intensity measurements
- 3.5 Photoluminescence geometry a) 45° and b) 90°
- 4.1 Photoluminescence spectra at 300, 100 K and 4.2 K
- 4.2 PC spectra of Sample 1 at RT (I) and 100 K (II)
- 4.3 PC spectra of Sample 2 at RT (I) and 100 K (II)
- 4.4 PC spectra of Sample 3 at RT (I) and 100 K (II)
- 4.5 PC versus intensity (low light) for Sample 1 a) RT and b) 100 K
- 4.6 PC versus intensity (low light) for Sample 2 a) RT and b) 100 K
- 4.7 PC transient versus intensity at $\lambda = 490$ nm (high light) for Sample 3
a) RT and b) 100 K (normalized)
- 4.8 PC transient versus intensity at $\lambda = 600$ nm (high light) for Sample 3
a) RT and b) 100 K (normalized) c) PC transient raw data.
- 4.9 Photocurrent versus intensity at $\lambda = 600$ nm for Sample 1 at RT (\bullet) and 100 K (\circ)
- 4.10 Photocurrent versus intensity at $\lambda = 600$ nm for Sample 1 at RT (\bullet) and 100 K (\circ)
- 4.11 Photocurrent versus intensity at $\lambda = 600$ nm for Sample 3 at RT (\bullet) and 100 K (\circ)
- 4.12 PL transient versus intensity at $\lambda = 490$ nm (high light) for Sample 3
a) RT and b) 100 K
- 4.13 Photoluminescence versus intensity for Sample 3 a) $\lambda_{\text{ex}} = 490$ nm and
b) $\lambda_{\text{ex}} = 600$ nm

LIST OF TABLES

- 1.1 Physical Properties of CdIn_2S_4
- 3.1 Dye Ranges and Power curves for CMX 4 laser
- 4.1 a) Position of the peaks in the PC spectra
b) Photo-electronic properties of CdIn_2S_4
- 4.2 Effect of increasing light intensity on PC response
- 4.3 Decay time of the PC transient at RT and 100 K for $\lambda = 490$ nm
- 4.4 Rise time of the Photocurrent response at RT and 100 K for $\lambda = 490$ and 600 nm

ABBREVIATIONS

CB:	conduction band
CW:	continuous wave excitation
e^- :	electron
f:	volume rate of generation of free electrons and free holes
fcc:	face centered cubic
h^+ :	hole
I_L :	light intensity
I_p :	photocurrent
LNT:	liquid nitrogen temperature
O.D.:	optical density
PC:	photoconductivity
PL:	photoluminescence
PM:	photomultiplier
PPS:	pulses per second
RT:	room temperature
VB:	valence band

I INTRODUCTION

1.1 Origin of the project.

The discovery of the semiconducting properties of the III-V compounds opened up a new world in semiconductor research. Very rapidly, the conditions necessary for the occurrence of semiconductivity in these alloys were recognized and an intensive search for new semiconductors began. Unfortunately, the problems of controlling composition, crystalline perfection and purity, and hence the physical properties of the material increase markedly with the number of components and limit the applicability of this type of compound.

In the past few years a great deal of research has been focused on the analysis of the properties of the family of ternary compounds, $A^{II}B_2^{III}X_4^{VI}$ (where A = Zn, Cd or Hg ; B = Ga or In ; X = S, Se or Te) and in particular, $CdIn_2S_4$. Features characteristic of this series of compounds include the absence of any excitonic structure in the low temperature optical spectra^(1,2,3), a large degree of intrinsic disorder, the observation of radiative recombination between localized levels only⁽⁴⁾ and the presence of a continuous distribution of electron trapping levels⁽⁵⁻⁹⁾.

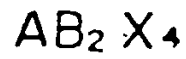
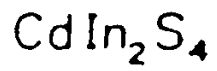
The high density of levels localized in the gap, originating from the presence of structural disorder within the lattice, has been proposed as the origin of these characteristics. The study of photoluminescence (PL)^(6,9-16) and photoconductivity (PC)^(8,16-23), coupled with systematic changes in crystal preparation, have been used for the detection and

characterization of localized levels and for the analysis of their nature and properties.

The fundamental optical properties of CdIn_2S_4 have been widely analysed by means of absorption⁽²⁴⁻²⁶⁾, reflectivity⁽²⁾ and photoemission⁽²⁷⁾ measurements. Band structure calculations have also been performed for this compound⁽²⁸⁾.

CdIn_2S_4 has an indirect band gap energy of $E_g^i = 2.28 \text{ eV}$ at room temperature (RT)⁽²⁹⁾ and 2.45 eV at liquid nitrogen temperature (LNT) and its direct transition occurs at 2.62 eV at RT. At temperatures up to 403 K , the crystal has a partially inverted spinel structure; that is Cd and In atoms are capable of occupying both tetrahedral and octahedral sites. Above this temperature, an order-disorder transition occurs in the cation sublattice of the crystal^(2,30) and the structure is less well defined. Figure 1.1 shows a quarter of a face centered cubic (fcc) spinel unit cell in which open circles are A-site atoms, the larger closed circles are B-site atoms, and the smaller closed circles are X-site atoms in the $\text{A}^{\text{II}}\text{B}_2^{\text{III}}\text{X}_4^{\text{VI}}$ molecular formula.

Although the physical properties of CdIn_2S_4 , summarized in Table 1.1, are relatively well known, very little basic research has yet been done using intense laser excitation in the study of processes such as photoconductivity, optical absorption and photoluminescence. Kinetics, involving the lifetime of excited states as influenced by the population of impurity levels, plays an important role in the three aforementioned processes. In fact very little is known about the kinetics of excited carriers in CdIn_2S_4 at either low or high excitation intensities.



○ A-Site (Cd, +2)

● B-Site (In, +3)

• X atom

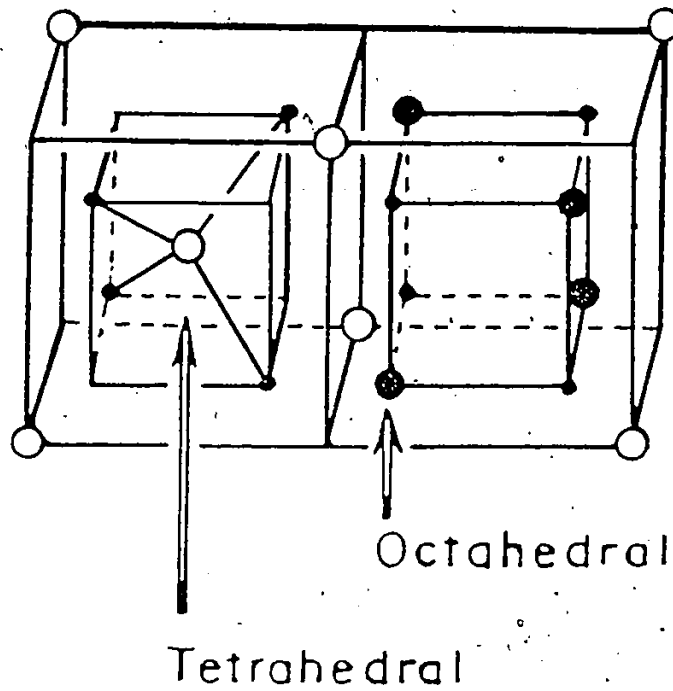


Figure 1.1 A quarter of the fcc spinel unit cell

Table 1.1 Physical Properties of CdIn_2S_4 (a)

Crystal Symmetry	Cubic Spinel
Lattice Constant	10.8 \AA
Energy gap	RT = 2.28 eV LNT = 2.45 eV
Refraction coefficient (n)	2.55
Effective mass of electron (m^*)	$0.17 m_0$
Hall mobility (μ_H)	$200 \text{ cm}^2/\text{V-sec}$ at RT
Phase transition temperature	130°C
Melting point	1105°C

(a). Table adapted from reference 31.

An exploration of the kinetics of excited carriers will form the major part of this thesis.

1.2 Summary of the project.

The present work concerns, in part, the spectral response of the PC and the dependence of this response on light intensity. The spectral response of the photocurrent of $\text{CdIn}_{24}\text{S}_4$ at 100 K and 300 K in the 400 to 700 nm excitation range was investigated to determine both the energy gap and the position of the impurity levels present within the gap. The latter parameter is related to the degree of disorder in the semiconductor. From this analysis it will also be possible to quantitatively deduce the relative density of these impurity levels between the different samples studied.

The dependence of the intrinsic and extrinsic PC will then be studied as a function of light intensity (Lux-Ampère experiment) over twelve orders of magnitude at both temperatures. A monochromator will be used for the low intensity excitation source and a pulse laser for the high intensity excitations. Information determined from this intensity dependence, coupled with the knowledge of the impurity behaviour in the case of laser excitation and the time variation of the PC transient will be used in the analysis of the kinetics of the photoexcited carriers.

Two interesting features were observed in the Lux-Ampère experiments: 1) Sublinearity and linearity dependence of the photocurrent (I_P) on excitation intensity (I_L) ($I_P = KI_L^x$, where $\frac{1}{2} < x < 1$) at both low and

high intensities of illumination in the intrinsic and some extrinsic regions, and;

ii) saturation of the photocurrent, I_p , at high light intensity, I_L , in the extrinsic region 590-610 nm. The saturation of impurity-induced photoconductivity by intense light was extensively studied and proved to be a very complex problem. This saturation effect provides useful information about deep impurity levels in semiconductors⁽³²⁾. Saturation of the PC in some CdIn_2S_4 crystals was observed at intensities of 10^9 W/m^2 at 600 nm and this allowed for determination of the density of the levels responsible for the absorption in CdIn_2S_4 at that wavelength. (These results have been published in Physical Review B 15, 1985, in press).

It is possible that this saturation effect may also be seen in the dependence of the absorption coefficient on the intensity of excitation. Knowing that the PC is proportional to both the coefficient of absorption, α , and the carrier lifetime (vide infra), τ , saturation of the photocurrent at high intensities would involve a decrease in the absorption coefficient if the lifetime of the photoexcited carriers remain constant.

The project also involves the analysis of the photoluminescence emission spectra as a function of temperature. The reasons for this study are twofold; firstly, to determine whether the samples studied follow the reported band diagram proposed for CdIn_2S_4 ⁽¹³⁾ and secondly to characterize the radiative recombination processes by which carriers decay. Finally some preliminary results on the dependence of the PL intensity and PL transient on the intensity of excitation in the intrinsic and extrinsic regions will be reported. In these experiments, very interesting results

were obtained, particularly in the case of PL versus intensity at high excitation intensity where a saturation effect was again seen. Measurements of this effect, coupled with a close analysis of the PL transient and thus, the PL transient kinetic processes involved, allow for the assignment of this saturation effect to an emptying of impurity levels at high light intensity. This emptying of levels suggests an inversion of population between two of the levels present in the gap. Such population inversion coupled with the observation that the recombination process between these two levels is a radiative one, suggests an application of CdIn₂S₄ crystals in laser physics.

1.3 Scheme of the thesis.

The first part of the thesis describes the theory required for the analysis of the results and is based on the work of Rose⁽²³⁾ and Bube⁽³⁴⁾. A short introduction to the phenomenon of photoconductivity will be followed by some significant theoretical models relating to our CdIn₂S₄ band diagram. These models will provide a basis for the explanation of the results obtained in the PC versus intensity measurements. A short introduction on photoluminescence process will open a new section. As previously discussed, measurements of luminescence provide useful information about critical steps in the mechanism of PC. The relationship between PL and PC will be described. This section will end with a full investigation of the proposed energy band diagram for CdIn₂S₄.

Chapter III will be concerned with the experimental techniques. The final, and most important chapter, will give the essential aspects of the experimental results and is divided into five sections;

- 1) Photoluminescence spectra;
- 2) Photoconductivity spectra (at low light intensity);
- 3) PC versus intensity of excitation (at low and high intensities);
- 4) Absorption versus intensity of excitation; and
- 5) Photoluminescence intensity and PL transient versus intensity of excitation

The experimental results and the discussion of these results will be given in each section. A discussion of the possible application of this work for future development in semiconductor research will conclude this thesis.

II. THEORY

The term "photoconductivity" covers all the phenomena by which the conductivity changes, increasing or decreasing, following absorption of light in the material under study. PC is not an elementary process but includes several successive or simultaneous mechanisms including optical absorption, hot carrier relaxation, charge carrier transport and recombination. When the recombination or capture process terminating PC is radiative, luminescence emission results. Luminescence is, therefore, the inverse process of absorption.

Thus, although PC is in general quite a complex phenomenon to understand, it offers a means of studying many of the physical properties of the material. For example, the spectral dependence of PC provides information on the energetic position of the impurity levels.

This present chapter is divided into four sections. The first section gives, in general terms, a description of PC. The lifetime of excited carriers and the trapping phenomena will also be discussed. The second section considers, in detail, a theoretical model for linear and sublinear dependence of the magnitude of the photocurrent on the excitation intensity. The third part will be dedicated to the explanation of the basic processes of photoluminescence and the relation of this phenomena to PC. Finally, the band diagram of CdIn_2S_4 will be discussed in detail. The origin of each impurity level inside the gap will be discussed in terms of the diagram.

2.1 General description of PC phenomena

In this section details of electronic processes directly connected with the photoconductivity mechanisms found in crystals will be explained. The principal purpose of this section is to introduce the parameters necessary for a simple description of PC.

A. General mechanisms:

The observation of any PC phenomenon requires the presence of at least one type of mobile charge carrier. In general, the conductivity due to these charge carriers can be expressed as:

$$\sigma = e [n \mu_e + p \mu_p] \quad (2.1)$$

where e is the magnitude of the electronic charge, μ_e (μ_p) is the electron (hole) mobility and n (p) is the concentration of free electrons (holes). The PC or the variation of electron (hole) conductivity upon light irradiation, has the general form

$$\Delta\sigma = e [\Delta n \mu_e + n \Delta\mu_e + \Delta p \mu_p + p \Delta\mu_p] \quad (2.2)$$

where Δn (Δp) is the number of free electrons (holes) created by the exciting light and $\Delta\mu_e$ ($\Delta\mu_p$) the variation of the electron (hole) mobility due to the exciting light. Thus, PC may arise from a change in the carrier concentration and/or carrier mobility. Let us make the assumption that $\Delta\mu_e$ and $\Delta\mu_p$ are both zero. This is a fair approximation since, in the temperature range studied (100-300 K), both the phonon scattering mechanism which is the dominant scattering process at high temperature ($\mu \propto T^{-3/2}$) and the charge impurity scattering which is dominant at low temperature ($\mu \propto T^{3/2}$) are both important so that over the temperature range studied μ

varies by less than a factor of 2 as demonstrated by Emdo et al. (38)

Equation 2.2 can thus be re-written as

$$\Delta\sigma = e [\Delta n \mu_e + \Delta p \mu_p] \quad (2.3)$$

Two processes may influence the values of Δn and Δp ; the creation of electron-hole pairs and the recombination processes. The next two sections will discuss in greater detail these two opposing processes.

B. Free carrier creation.

Free electrons (holes) can be produced by optical excitation of electrons (holes) from the valence (conduction) band states or impurity states to the conduction (valence) band. In general, two regions of a PC spectra must be considered: the low absorption ($\alpha d \ll 1$) and high absorption ($\alpha d > 1$; $\alpha > 10^3 \text{ cm}^{-1}$) regions. In the low absorption region, carriers are generated over the entire thickness, d , of the sample and the generation rate is proportional to the absorption coefficient α . This region is attributed to extrinsic excitation where electrons (holes) are excited from impurity states (of which there is a low density) to the conduction (valence) band. So, transitions in the low absorption region generally produce only one type of free carriers. For example, the electron transitions from acceptor levels to conduction band are in the low absorption region. This transition in particular was studied in the PC versus intensity experiment as will be described in chapter 4.

In the high absorption region, light is absorbed in a very thin layer below the surface. This transition corresponds to band-to-band excitation. One of the most important results obtained from the present measurements is the density of acceptor levels in CdIn_2S_4 samples. This will be discussed in more detail in chapter 4. We will presently derive a relation between the number of photons absorbed in both the low and high absorption regions and the incident photon flux.

In the PC experiment, the specimen with rectangular plane faces and uniform thickness, d , is oriented such that the exciting light falls perpendicular to one of the plane faces. Let I_L represent the intensity of radiation; i.e., the incident power per unit area on a surface. If I_L' is the intensity in the material, then the power absorbed per unit volume per unit time is equal to $\alpha I_L'$, where α is the absorption coefficient. The number of free electrons produced per unit volume per unit time is then equal to $q\alpha I_L'/h\nu$ where q is a constant known as the quantum efficiency. If $R I_L$ is the intensity of the reflected radiation, and $T I_L$ is the intensity of the transmitted radiation, it may be shown that⁽³⁴⁾

$$R = R_o \left\{ 1 + \frac{(1-R_o)^2 e^{-2\alpha d}}{1-R_o^2 e^{-2\alpha d}} \right\} \quad (2.4)$$

and

$$T = \frac{(1-R_o)^2 e^{-\alpha d}}{1-R_o^2 e^{-2\alpha d}} \quad (2.5)$$

where R_0 is the reflection coefficient at the surface of the sample. The total amount of radiation absorbed by the sample per unit time is equal to $I_L (1-T-R)$, and if $\alpha d \ll 1$ (extrinsic region), then the average rate of absorption per unit volume is equal to $I_L (1-T-R)/d$. Using equation 2.4 and 2.5, we have $(1-T-R) \rightarrow \alpha d$ when $\alpha d \ll 1$ (see appendix A) and the radiation is uniformly absorbed throughout the sample at a rate αI_L per unit volume. The rate of formation of $e^- - h^+$ pairs, f , is then given by the equation

$$f = q \alpha I_L / h\nu \quad (2.6)$$

If, on the other hand, $\alpha d \gg 1$ (intrinsic region), the intensity just inside the illuminated surface is given as $I_L' = I_L (1-R_0)$, as there is no appreciable radiation reflected from the back surface. In this case,

$$I_L' = I_L (1-R_0) e^{-\alpha x} \quad (2.7)$$

and the rate of pair creation, f , is given by

$$f = q \alpha I_L (1-R_0) e^{-\alpha x} / h\nu \quad (2.8)$$

where x is the thickness at which all the radiation is absorbed. These equations will be relevant in the evaluation of the density levels present in CdIn_2S_4 crystal.

C. Recombination mechanisms

As previously discussed, the change in conductivity resulting from excitation is normally terminated by the recombination of the photoexcited

electrons and holes. It is therefore the recombination process which determines the lifetime of free carriers and it is clearly impossible to discuss PC without mentioning the basic concepts of recombination.

Recombination can occur through various mechanisms and are classified according to the answers to the following two questions:

- 1) Is the recombination direct or through an imperfection?
- 2) How is the energy of the excited carriers dissipated in the recombination?

Recombination can occur both by the direct recombination of free electrons and holes (band-to-band) without one of the carriers being first captured at an imperfection, or by the recombination of a free carrier of one type with a bound carrier of the opposite type, previously captured at an imperfection in the crystal. In general, recombination through an imperfection dominates for low-carrier densities, and direct (band-to-band) recombination becomes important only for high-carrier densities.

Whenever recombination between photoexcited electrons and holes occurs, some means must be provided for the dissipation of the excess energy of the excited carriers. There are three basic ways in which this energy dissipation can occur:

- 1) by the emission of photons (radiative recombination), the energy of each photon being equal to the energy difference between the two carriers before recombination. (This kind of recombination gives rise to the luminescence process as will be discussed later);
- 2) by the emission of a number of phonons (non-radiative) with total energy equal to the excess energy to be dissipated; and,

3) by a three-body collision, the excess energy being given up to a third carrier in what is called an Auger recombination.

Two or more of these processes may be involved simultaneously. Another way by which PC may be interrupted is by the capture of free carriers by trapping centers. The next section will provide a qualitative discussion of traps.

Since the lifetime of free carriers is determined by the recombination processes, the lifetime can be considered as one of the key parameters for an understanding of photoconductivity. The term "lifetime", has been used to describe a number of different quantities (such as: Free lifetime, excited lifetime, pair lifetime, minority carrier lifetime and majority carrier lifetime)⁽³⁴⁾ and it is therefore necessary to examine the concept in some detail.

If light falling on a photoconductor, creates f electron-hole pairs per second per unit volume of the photoconductor, then in steady state:

$$f \tau_n = \Delta n \quad (2.9a)$$

and

$$f \tau_p = \Delta p \quad (2.9b)$$

where τ_n and τ_p are the free lifetimes of an electron and hole, and Δn and Δp are, respectively, the additional free electron and hole densities present as a result of absorption of light. The free lifetime is the time that the charge carrier is free to contribute to the conductivity.

To put it another way, it is the time that an excited electron spends in the conduction band, or the time that an excited hole spends in the valence band.

The free lifetime of a charge carrier can be

- a) terminated by recombination;
- b) interrupted if the carrier is trapped, to be resumed when the carrier is freed from the traps; or,
- c) undisturbed if the carrier is extracted from the crystal by the field at the same time as an identical carrier is injected into the crystal from the opposite electrode.

From equations (2.9), it is possible to re-write equation (2.3) in the following way:

$$\Delta\sigma = fe (\mu_e \tau_n + \mu_p \tau_p) \quad (2.10)$$

This relationship illustrates why the lifetime is one of the key parameters in PC.

The lifetime of photoexcited carriers is a function of the following two parameters; the density of recombination centers, and their capture cross sections. Let there be only one type of impurity - a recombination centre. Let p_r be the density of centers unoccupied by electrons and n_r the density of centers occupied by electrons. Let S_n be the capture cross section of an unoccupied center for free electrons and S_p the capture cross section of an occupied center for free holes. Let the material be exposed to light whose energy is larger than that of the band gap. The volume rate of generation of free electrons and free holes is designated, as before, by f . We further assume that the densities Δn and Δp of excited carriers are both small in comparison with n_r and p_r . With these assumptions (2.9) can

be re-expressed as

$$\Delta n = f \tau_n = \frac{f}{p_r v S_n} \quad (2.11a)$$

$$\Delta p = f \tau_p = \frac{f}{n_r v S_p} \quad (2.11b)$$

For simplicity, the thermal velocity v of free electrons and of free holes are assumed to be equal. The lifetime of a free electron

$$\tau_n = \frac{1}{p_r v S_n} \quad (2.12a)$$

is independent of and, consequently, in general not equal to the lifetime of a free hole

$$\tau_p = \frac{1}{n_r v S_p} \quad (2.12b)$$

These expressions for lifetime are derived from the concept that in the time, τ_n , an electron to which the cross-sectional disk, S_n , is attached will trace out a volume $\tau_n v S_n$ equal to the volume p_r^{-1} associated with a capturing center. Different types of impurity centers may have different densities and different cross sections. In this case $\tau_n^{-1} = \sum_i v p_i S_i$. Equation 2.12a shows that changing the density of centers unoccupied by electrons (p_r) changes the free electron lifetime (τ_n); τ_n is not constant. Optical excitation can change the density of unoccupied centers and hence change the lifetime. The steady state PC has been observed in different materials to be any of a superlinear, sublinear or linear function of incident intensity. At low intensities the excitation rate f is a linear function of incident intensity. Hence equation 2.11 tell us that τ must be

a non-linear function of intensities. A superlinear variation corresponds to τ increasing as a function of intensity; a sublinear variation corresponds to τ decreasing as a function of intensity.

Section 2.2 presents a model for τ either being independent of intensity or τ decreasing as a function of intensity. Hence it explains either a linear or sublinear variation of PC with intensity. This was what was observed in CdIn_2S_4 as will be discussed in chapter 4.

D. Qualitative effects of trapping.

Trapping is a fundamental process for energy storage in almost all electronically active solids. This energy storage is accomplished by the spatial localization of an excited electron or hole in such a way that the electron or hole is prohibited from moving freely through the crystal unless supplied with thermal or optical energy. When the trapped electron or hole is released, it is free to move until captured by a recombination center or by another trap. Those regions of the crystal which are able to capture electrons and holes, and detain them in a restricted volume, are called traps.

It has become a common practice in semiconductor terminology to refer to any center capable of capturing an electron or hole as trap. However, we will reserve the names "trap" and "trapping" for centers and processes which are determined by thermal equilibrium exchange with the

nearest allowed band. Thus we distinguish between trapping centers, the occupancy of which is determined by thermal equilibrium processes, and recombinations centers, the occupancy of which is determined by recombination kinetics. Because of this type of definition, there is an inherent vagueness in determining what types of centers are traps; in fact, any center can be a trap under one condition of light intensity and temperature, and a recombination center under another. It is convenient to define the location of a demarcation level, separating trapping and recombination levels, in the following way: when an electron (hole) is located at the electron (hole) demarcation level, it has equal probability of recombining with a free hole (electron) and of being thermally ejected to the conduction (valence) band. The occupation of a level lying above the electron demarcation level is determined by the conditions of thermal equilibrium between the levels and the CB; similarly, the occupation of a level lying below the hole demarcation level is determined by the conditions of thermal equilibrium between the levels and the valence band. The occupation of levels lying between the electron demarcation level and the hole demarcation level is determined by the recombination kinetics of the material.

The major effect of trapping is to make the experimentally observed decay time of the photocurrent after excitation has ceased, longer than the carrier lifetime. If no trapping centers are present, then the observed photocurrent will decay in the same way as the density of free carriers and the observed decay time will be equal to the carrier lifetime. If trapping centers are present but the free carrier density is much greater than the

density of trapped carriers, the observed decay time of the photocurrent will again be equal to the carrier lifetime. But if the density of free carriers is either comparable to or less than the density of trapped carriers, the thermal freeing of trapped carriers can prolong the decay so that the observed decay time is longer than the actual recombination determined lifetime of a free carrier. In the extreme case, in which the density of trapped carriers is much greater than the density of free carriers, the entire photocurrent decay is dominated by the rate of traps emptying rather than by the rate of recombination.

The reason for talking about trapping centers is that CdIn_2S_4 crystals contain a continuous distribution of electron trapping levels. The origin of these traps will be given in the last section of the theory. From the PC versus intensity measurements, it will be possible to evaluate the density of these traps, a parameter which depends upon preparation conditions.

2.2 Theoretical model for linear and sublinear behaviour of PC versus intensity; $I_p = f^\alpha$ [$\frac{1}{2} < \alpha < 1$]^(*).

The variety of dependencies of photocurrent on light intensity and temperature is virtually unlimited. This statement is borne out

(*) In the equation $I_p = f^\alpha$, I_p represents the photocurrent and f the volume rate of generation of free electrons and free holes ($f/\text{sec-cm}^3$).

experimentally by the fact that photocurrent has been observed to increase linearly, supralinearly and sublinearly with increasing light intensities. Similarly, photocurrent has been observed to be insensitive to temperature as well as to increase or decrease with increasing temperature. If the creation rate of free carriers is constant then a non-linear dependence of the magnitude steady state PC is produced by an intensity dependent τ .

As mentioned in the introduction, a linear and sublinear behaviour of the PC versus light intensity of excitation has been observed in CdIn₂S₄ crystals. The model to be described in this section is the simplest type of model needed to account for the linearity and sublinearity dependence. The model used by Rose⁽³³⁾ to explain linear and sublinear behaviour to PC versus intensity will be used to explain similar behaviour in CdIn₂S₄.

The model is represented in figure 2.1. In the diagram, N_t represents the density of empty traps; N_r , the density of recombination centers; p_r the density of such centers unoccupied by electrons and n_r , the density of centers occupied by electrons (i.e. $n_r + p_r = N_r$). In addition, E_f represents the dark Fermi level; E_{fn} (E_{fp}), the steady state Fermi level for electrons (holes) and D_n (D_p), the electron (hole) demarcation level. As previously mentioned, the electron demarcation level is the level at which the probability of an e^- being excited thermally in the CB is equal to the probability of a free h^+ being captured at the level.

In the present model, two assumption are being made: 1) all the recombination centers are occupied in the dark ($n_r = N_r$), 2) the N_t states have an exponential distribution in energy such that

$$N_t(E_t) = A \exp \left[\frac{-(E_c - E_t)}{kT_1} \right] \quad (2.13)$$

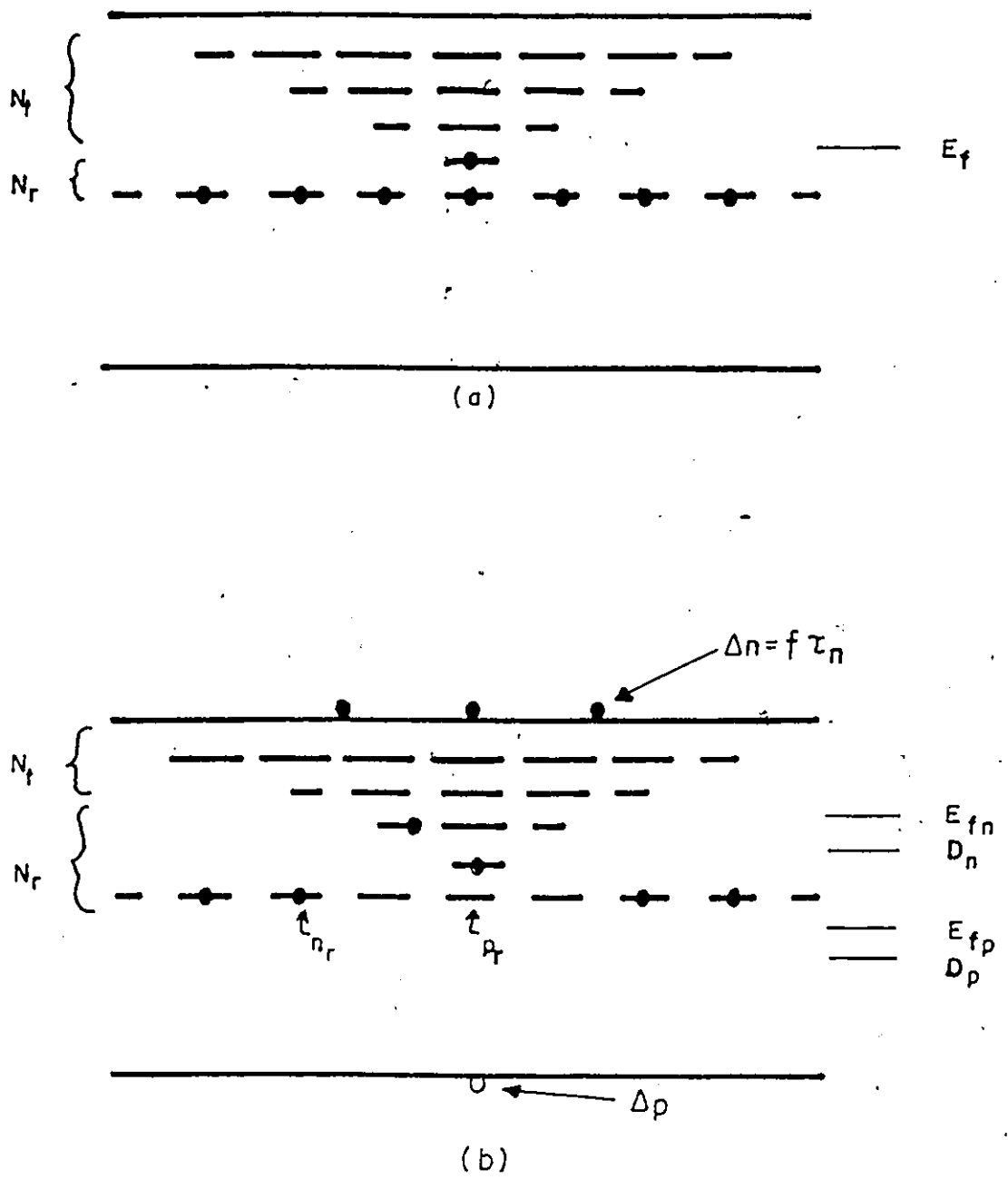


Figure 2.1 Model for exponents of current-light curve lying between 0.5 and 1.0
 a) Unilluminated ; b) Illuminated

where E_c and E_t are the energy at the CB and the trap level. The temperature, T_1 , is a parameter that can be adjusted to make the density of states vary more or less rapidly with energy below the CB. In the present discussion $T_1 > T$, where T is the ambient temperature. For convenience, let the capture cross sections of the N_t states be the same as those for the N_r states. Actually, the capture cross sections of the N_t states may differ markedly from those of the N_r states without affecting the main argument. Let us take the capture cross section of an unoccupied center for free e^- (S_n) to be much smaller than the capture cross section of an occupied center for free holes. By this assumption, the density of photoexcited electrons is much larger than that of photoexcited holes, i.e. $\Delta n \gg \Delta p$. Figure 2.1b shows the conditions at some intermediate light intensity. E_{fn} and E_{fp} are the steady-state Fermi levels defined by the densities Δn and Δp . The demarcation levels, D_n and D_p , are shifted slightly down from E_{fn} and E_{fp} because $n_r \gg p_r$.

There is now a simple physical picture to account for exponents less than unity derived from the distribution of N_t states. As the light intensity is increased, more and more of the N_t states are converted from trapping to recombination states. This conversion takes place as the steady-state Fermi level E_{fn} sweeps through the N_t states towards the CB. As p_r , the density of recombination states for electrons, increases with light intensity, the electron lifetime decreases, that is $\tau \propto f^{-\beta}$, therefore, $\Delta n = f\tau = f^{1-\beta}$. This decrease in the electron lifetime with increasing light intensity was observed experimentally and will be discussed in more detail in chapter 4.

To a good approximation, the density of empty states p_r produced by optical excitation is given by the number of N_t states lying between the original Fermi level, E_f , and the steady-state Fermi level, E_{fn} . These N_t states, were originally empty states that have now been brought into the category of recombination centers. The density of empty states, p_r , can be estimated in the following way:

$$\begin{aligned}
 p_r &= \int_{E_f}^{E_{fn}} N_t(E) dE \\
 &= \int_{E_f}^{E_{fn}} A \exp \left[\frac{-(E_c - E)}{kT_1} \right] dE \\
 &= kT_1 N_t(E_{fn}) \quad (2.14)
 \end{aligned}$$

From the above result, we can re-write equation 2.11a:

$$\Delta n = f \tau_n = f \left(\frac{1}{p_r v S_n} \right)$$

where v is the thermal velocity of the electron in the CB.

Substituting equation 2.14 into 2.11a:

$$\Delta n = f \frac{1}{kT_1 A \exp \left[\frac{-(E_c - E_{fn})}{kT_1} \right] v S_n} \quad (2.15)$$

and by definition we know that

$$\Delta n = N_c \exp \left[\frac{-(E_c - E_{fn})}{kT} \right]$$

$$= N_c \exp \left[\frac{-(E_c - E_{fn})T_1}{kT_1 T} \right] \quad (2.16)$$

where N_c is the effective density of states in the CB.

$$(N_c = 2 \left(\frac{2\pi m^* kT}{h^2} \right)^{3/2} = 10^{19} \text{ cm}^{-3} \text{ for } m^* = m \text{ at } T = 300 \text{ K}).$$

Insertion of equation 2.16 into equation 2.15 leads to

$$\Delta n = \left[\frac{f N_c^{T/T_1}}{kT_1 A v S_n} \right] T_1 / (T + T_1) \quad (2.17)$$

Since $T_1 > T$, the exponent $T_1 / (T + T_1)$ lies between 0.5 and 1.0.

We have in equation 2.17 a simple mechanism to account for photocurrents that increase with increasing light intensity as any power lying between 0.5 and unity. While the model assumes an exponential distribution of states lying between E_f and E_c , the distribution extends only over the small range of energies through which E_{fn} moves since the largest contribution to p_r comes from states near E_{fn} . Further, the distribution need only be approximated by an exponential form over this short range of energies. Hence, almost any distribution of states will lead to exponents of the current-light curve lying between 0.5 and unity. As the distribution of states becomes more constant in energy, the characteristic temperature, $T_1 \rightarrow \infty$ and Δn varies more nearly linearly with light intensity.

From this discussion we see that an exponent lying between 0.5 and unity requires a distribution of states in energy and that the appearance

of exponents between 0.5 and 1.0 provide strong evidence for a continuous distribution of states. In this argument, the mobility and capture cross sections are assumed to be constant and the photoconductor homogeneous. Bube⁽³⁴⁾ has shown that, in some cases, the mobility varies with light intensity owing to a change on the discrete states and a consequential change in the scattering of the charged centers. The variation of mobility must, of course, be divided out before testing the above model.

In the present argument, it was assumed that the light induced transition of electrons from the VB to the CB gives rise to free pairs. Owing to the higher density and larger capture cross section of the n_r states, the free holes are rapidly captured into the recombination states leaving the free-electron density of major interest. It is clear that if the light was absorbed by the recombination (n_r) states initially, the holes would be generated directly in the recombination centers. The result would be the same as if the holes had been generated in the VB and rapidly captured into the recombination centers. In fact, this type of photogeneration makes the analysis even simpler and freer from approximation. For example, the steady-state Fermi level for electrons approximates even more closely the properties of a thermal equilibrium Fermi level, since the occupancy of the trapping states is controlled only by thermal exchange with the CB and is not perturbed by the capture traffic of free holes.

All the concepts explained in this section will provide a good guide in the understanding of the results of the Lux-Ampère experiments.

2.3 Photoluminescence

When the recombination or capture process terminating or interrupting PC is radiative, luminescent emission results. Luminescence is, therefore, the inverse process of absorption. This process may be further subdivided on the basis of the electron excitation mechanism. Excitation by an electric current results in electroluminescence, while excitation by optical absorption produces photoluminescence. Cathodoluminescence results when the excitation is produced by a high energy electron beam. Thermoluminescence occurs when the electrons are frozen at low temperature in their trapping states following excitation. Then, as the solid is heated, thermal agitation assists the electron to de-excite and release radiation.

Because luminescence is one of the processes which terminates PC, measurements of luminescence emission spectra on decay provide useful information about critical steps in the mechanism of PC.

The following general statements may be made about both PC and luminescence:

- 1) Good luminescent materials need not be photoconducting. Luminescence can result from processes in which the generation of free carriers is not involved.
- 2) Good photoconductors need not show luminescence. It is the long free lifetime of excited carriers which makes a good photoconductor.
- 3) In general, PC will be better in luminescent materials which exhibit

phosphorescence (i.e., slow non-exponential decay of emission after cessation of excitation) than in those which do not. The reason for this is that the occurrence of phosphorescence (implying the thermal freeing of trapped carriers) indicates that free charge carriers have been formed by the excitation process.

4) Good luminescent materials require rapid recombination, whereas good photoconductors require slow recombination.

5) It has been generally found that, in materials which show both luminescence emission and PC, the rate of decay of luminescence emission is appreciably more rapid than the decay of the PC.

Radiative recombination in semiconductors has been the subject of an enormous number of experimental and theoretical investigations which have proven fruitful for the development of our understanding of semiconductor physics. In addition these fundamental studies have given rise to interesting applications such as light emitting diodes and semiconductor lasers.

2.4 Energy band diagram of CdIn_2S_4

The model of the band diagram of CdIn_2S_4 for the PC excitation and recombination processes adopted in the present paper is the one proposed by Grilli et al.⁽¹³⁾ (Figure 2.2). This model incorporates the results of Anedda et al.⁽⁸⁾ which demonstrated the presence of a high density of

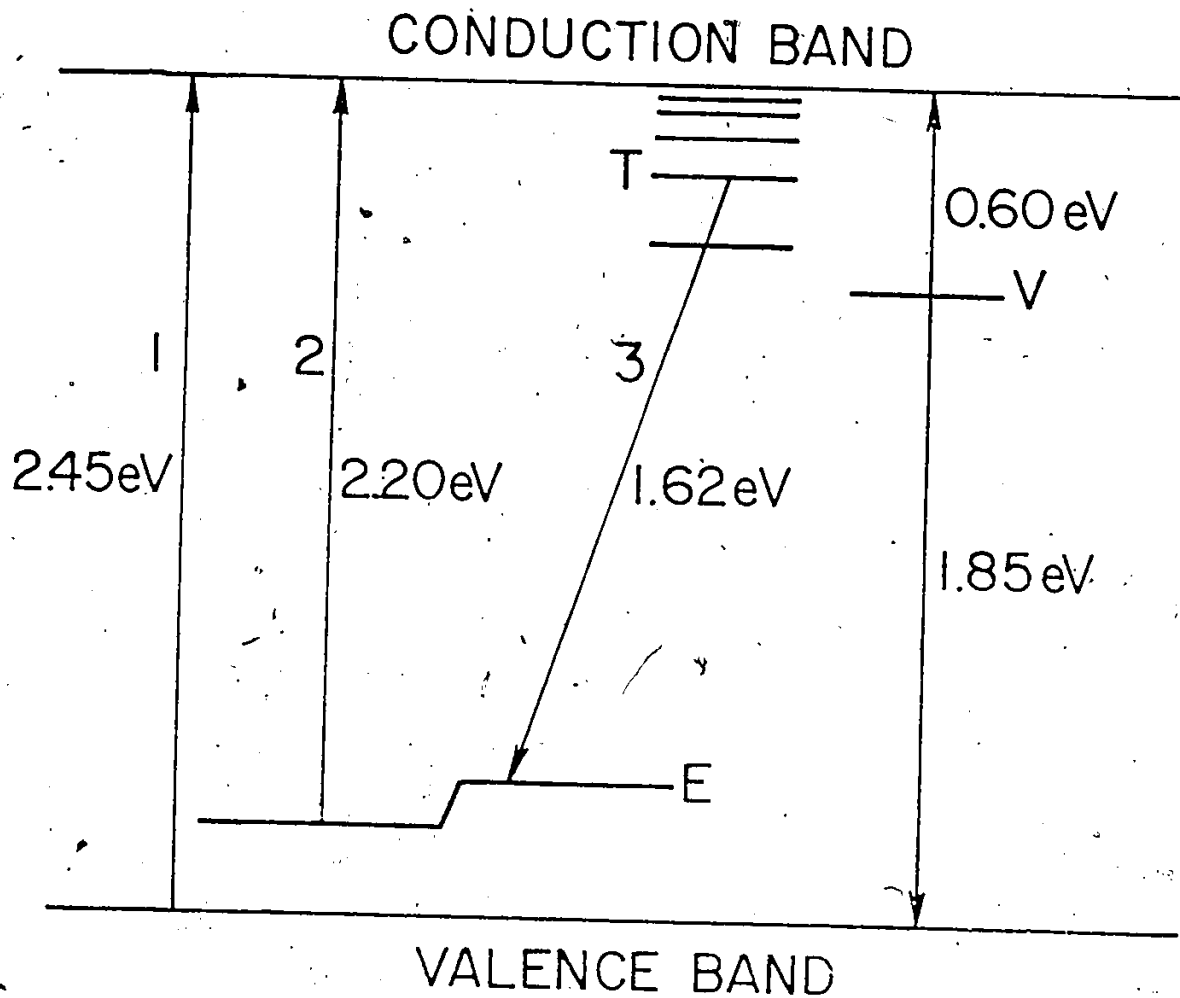


Figure 2.2. Energy-level scheme and model of recombination processes of photo-excited carriers in CdIn₂S₄ at LNT

electron trapping levels with an exponential distribution in energy and the presence of an acceptor level at 0.25 eV from the top of the valence band in CdIn_2S_4 crystals. The origin of these levels has been attributed to anti-structural defects due to In-Cd exchange probably induced by the phase transition from the partial inverse spinel structure (low temperature phase) to the disordered spinel structure (high temperature phase).

In regards to the electronic properties of the above defects, it follows from elementary considerations that an In atom in a Cd lattice site has one excess valence electron for the band formation and thus behaves as a donor; conversely, a Cd atom in an In lattice site behaves as an acceptor; therefore, each In-Cd exchange introduces both a donor and an acceptor. The compensation is therefore complete as the carriers of opposite sign recombine and all centers remain ionized. The acceptor position inside the gap⁽⁸⁾ is

$$E_a = E_v + 0.25 \text{ eV}$$

Because of the continuous electron trap distribution, the donor position can be given only as an average. The total number of electron traps was calculated to be $N_t = 9 \times 10^{19} \text{ cm}^{-3(8)}$, but 98% of the traps are shallow levels situated in the energy range 0 - 0.1 eV below the conduction band.

The presence of the continuous donor distribution and the discrete acceptor levels at 0.25 eV above the valence band in CdIn_2S_4 may appear surprising. This asymmetric behaviour may be due to the asymmetry of the

effective masses of electrons and holes, the latter being generally larger. Acceptors are thus more localized than donors and are more distant from the respective band⁽⁸⁾: the increase in the concentration broadens acceptor states less than donor states so that they cannot reach into the valence band.

In the present model, E will represent the compensated acceptors and T, the trap distribution. It is important to remember that all the traps and acceptors are ionized due to the fact that the Fermi level lies about 2.1 eV above the valence band⁽²³⁾. The V-center, placed at approximately 0.6 eV from the bottom of the conducting band, is attributed to sulfur vacancies. Later, it will be demonstrated that the V-centre plays no role in the recombination of free carriers at the temperatures studied (100 K to 300 K).

III EXPERIMENTAL TECHNIQUES

This chapter will describe, in detail, the techniques used in the investigation of the previously mentioned optical experiments; including, photoconductivity, photoluminescence and optical absorption. This section of the thesis should provide useful information for the researcher interested in pursuing this type of work.

3.1 Sample preparation.

$GdIn_2S_4$ single crystals of up to a few tens of cubic millimeters in volume were grown by the method of chemical vapour transport, using iodine as the transport gas, at the University of Cagliari, Italy. All samples were n-type with a conductivity at 300 K of about $10^{-5} \Omega^{-1} \text{cm}^{-1}$. Because of the very good quality of the crystal surfaces, no polishing or etching was necessary. PC spectra were obtained from smooth, natural surfaces of the crystals a fraction of a millimeter thick.

Photoconductivity and optical absorption were investigated at both room temperature (RT; 300 K) and 100 K, where liquid nitrogen was used, as determined by a Chromel-Alumel thermocouple. The photoluminescence was studied at a third temperature, 4.2 K, with the use of liquid Helium.

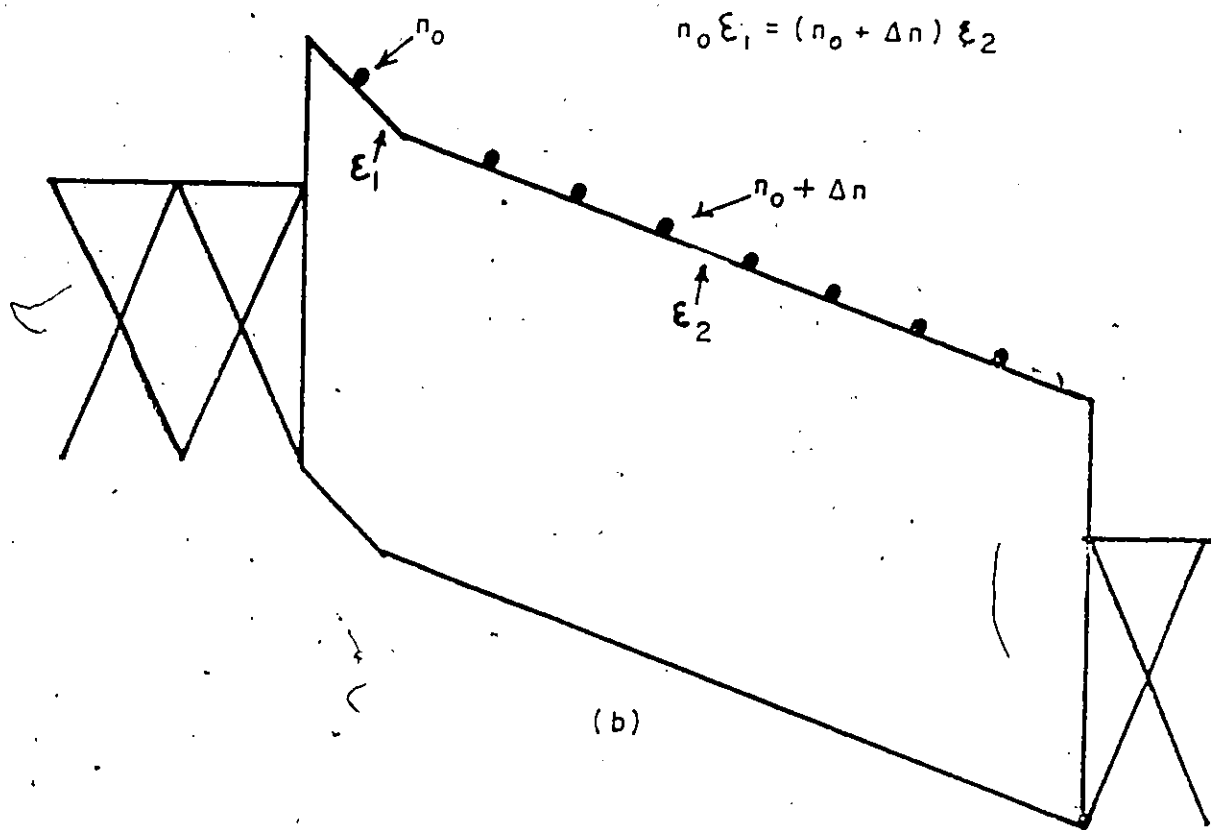
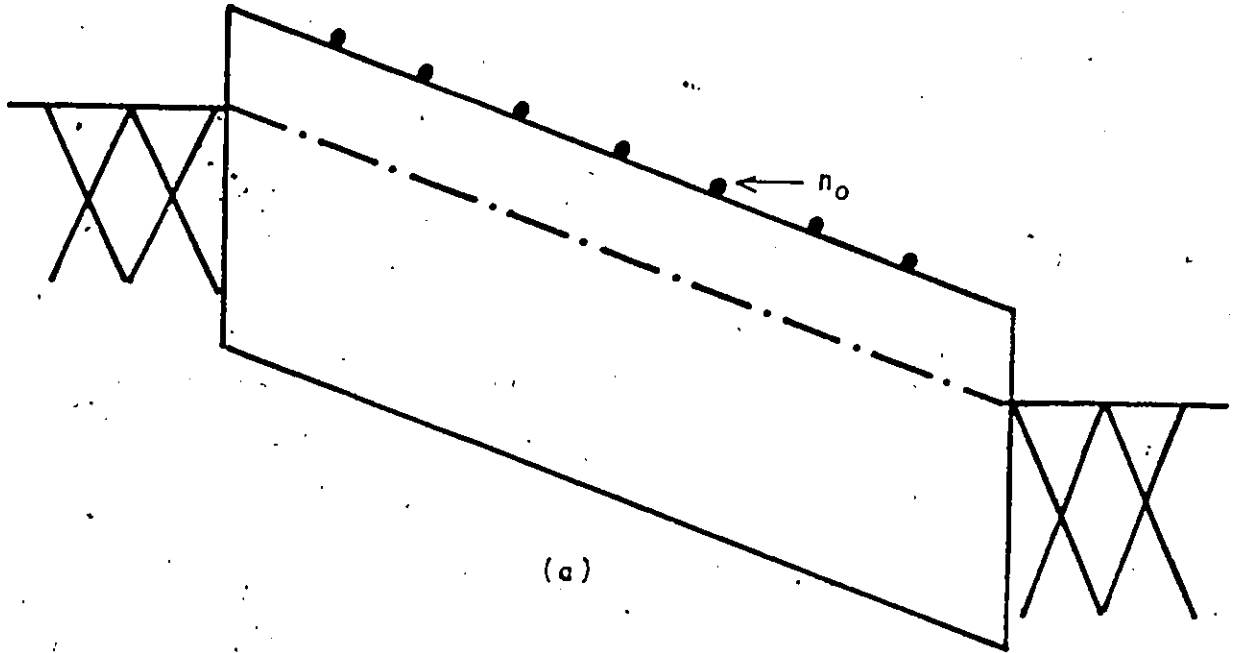


Figure 3.1 Representation of a neutral contact
 a) volume unilluminated
 b) volume illuminated

3.2 Relevance of good ohmic contact.

In order to measure the PC properties of a material, it is necessary to make electrical contact with the material by means of electrodes. Such electrodes would be considered ideal if they introduced no resistance to the flow of current, if they did not react chemically with the material, and if they were unaffected by variations in illumination, temperature or applied field strength. Although electric contacts to certain materials have been achieved with near to ideal properties, using specific electrode materials, there is still considerable art and uncertainty in choosing the proper electrode material to give an ideal contact with a new material.

The simplest metal-semiconductor contact is that shown in figure 3.1a. The conduction band remains flat out to the metal interface. The contact is called neutral in contrast to those contacts in which the bands bend up or down at the interface. The maximum current that can be drawn from a neutral contact is the thermionic emission from the metal over the potential step into the semiconductor. This maximum thermionic emission is equal to the random current from semiconductor to metal; hence, the thermionic emission will be saturated at a critical electric field in the semiconductor.

For field less than the saturating value, the current drawn through the semiconductor is less than that available from the metal and the contact is ohmic. It is ohmic in the sense that an increase in the field in the semiconductor will give a proportional increase in the current. It

is also ohmic in the sense that the contact can supply the additional current needed when the semiconductor is made more conducting by light. In the latter case, the effect of the added carriers, Δn , is to steepen the electric field at the contact in order to supply the additional current (see figure 3.1b). The range of photocurrents for which the contact is ohmic is limited to values less than the saturated thermionic emission. For light intensities higher than those needed to saturate the thermionic emission, the contact is said to be "blocking" (non-ohmic), that is, it supplies no additional carriers to replace those excited by the light in the volume of the semiconductor and drawn out at the anode. At these higher light intensities, the field becomes more and more concentrated near the electrode where the carriers enter, producing a non-linear variation of the PC response with light intensity.

In summary, an ohmic contact is one that supplies a reservoir of carriers freely available to enter the semiconductor as needed and we must experimentally ascertain that the contacts are ohmic under the entire range of light intensity used and the voltage applied to the Sample.

In the case of $\text{CdIn}_{2.4}\text{S}_4$, silver paint contacts proved to be ohmic in the temperature range studied (100 - 300 K) both under low intensity light including darkness and under high intensity light for applied voltages between 0 and 10 volts. Figure 3.2 shows the current-voltage (I-V) characteristics for sample 1 in the dark. The operating voltage for all the PC measurements was 9 volts. The silver contacts were deposited approximately 1 mm apart on the same crystal face. The current-voltage

Current vs Voltage

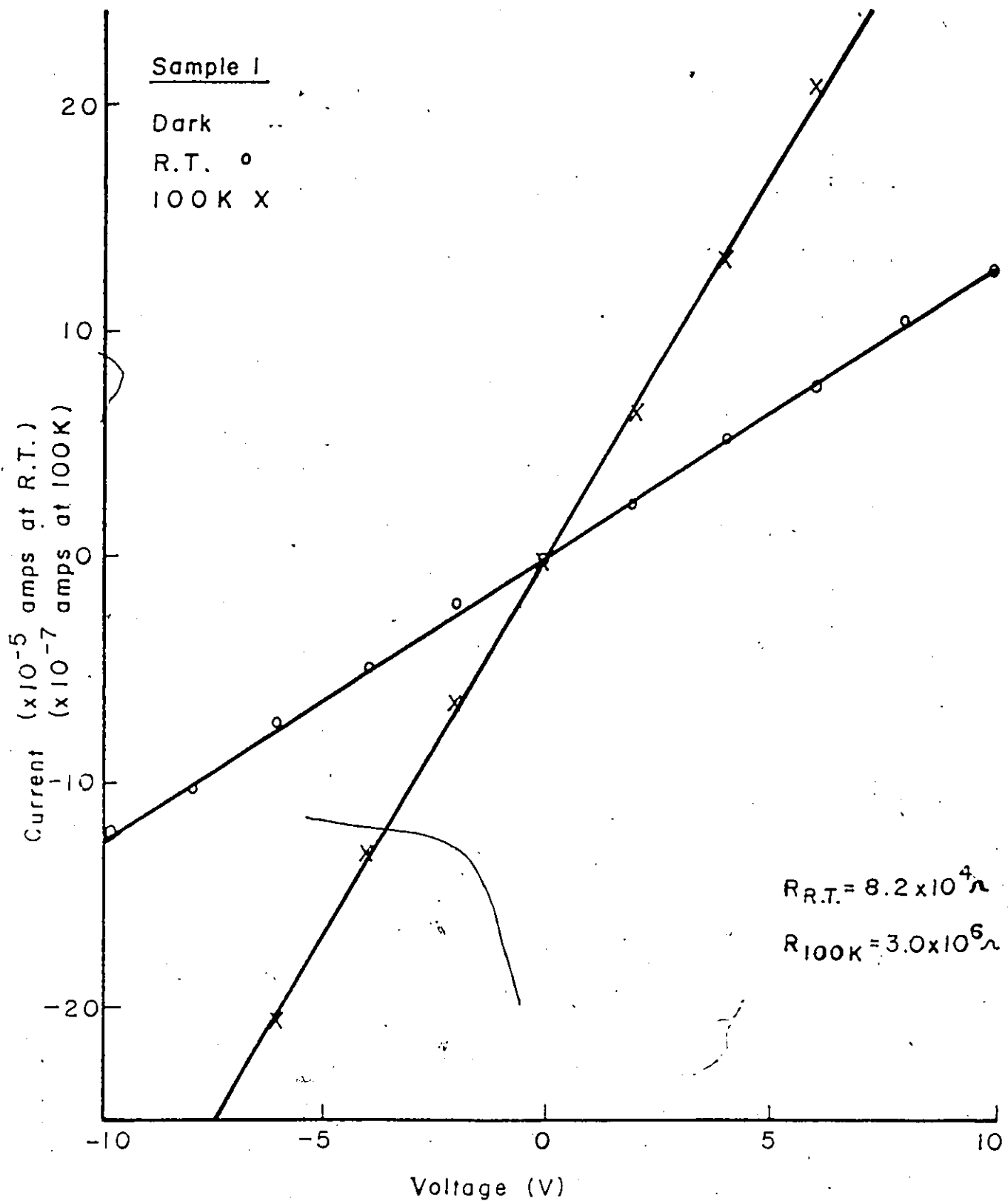


Figure 3.2 I-V characteristics at RT and 100 K in the dark (Sample 1)

curve was obtained by varying the voltage and measuring, simultaneously, the voltage drop between the contacts and the current passing through the crystal. The voltage was measured by a Keithley 155 microvoltmeter and the current by a Keithley 602 electrometer. The same detection technique, for the I-V experiment, was used for the low light intensity of excitation. The ohmicity of the contacts under high intensity excitation condition was demonstrated by shining the laser beam at the sample and recording the peak magnitude of the PC transient as a function of applied voltage. The relation was a linear, one, proving that the contacts were ohmic at these high intensities.

Having established the ohmicity of the contacts, we can turn to a discussion of the photoconductivity experiments.

3.3 Photoconductivity experiments.

A. Low light intensity PC.

CdIn_2S_4 samples, mounted on a plate on the cold finger of an optical cryostat under vacuum, were excited by a quartz-iodine lamp. The light was dispersed by a Bausch and Lomb monochromator which provided intensities of up to 2.5 W/m^2 . The resolution of the spectrometer was approximately 5 nm. The samples were always excited between the two ohmic contacts. The optical cryostat used was designed by Dr. E. Fortin and built at the University of Ottawa. Improvements were made in the method of making

electrical contacts to the samples. Before the modifications, the electrical connections from the outside to the inside of the cryostat were made by two insulated copper wires which went down to the top of the cold finger. Then two uninsulated copper wires were soldered to the insulated ones. The other end of the uninsulated wires were fixed by means of silver paint at the surface of the sample mounted on the cold finger. Unfortunately, when the temperature was dropped from 300 K to 100 K, the contacts at the surface of the sample often broke due to the length of the uninsulated copper wires and the thermal compression during the cooling process. Some modifications to the cryostat mounting scheme were necessary. Rather than placing the sample directly on the cold finger, a sample holder was designed in the hope of improving the contact strength (see figure 3.3a). The sample holder was made of copper plated circuit board and part of the copper was etched away with formic acid so that the sample could sit on an electrically insulating surface. Copper wires were then used to make the connections between the ohmic contacts of the sample and the electrodes on the plates. To fix the holder on the cold finger a simple "clip in" device was installed. Although this holder allows for greater freedom of manipulation of the samples and improved the strength of the contacts, relatively high temperatures were obtained at LNT due to the poor thermal contact between the sample and the cold finger.

PC spectra were recorded using a standard synchronous technique monitored with a lock-in amplifier. The chopping frequency was 44 Hz. The measuring circuit used in the PC experiment is shown in figure 3.3b. The photocurrent was detected by measuring the voltage drop across a load

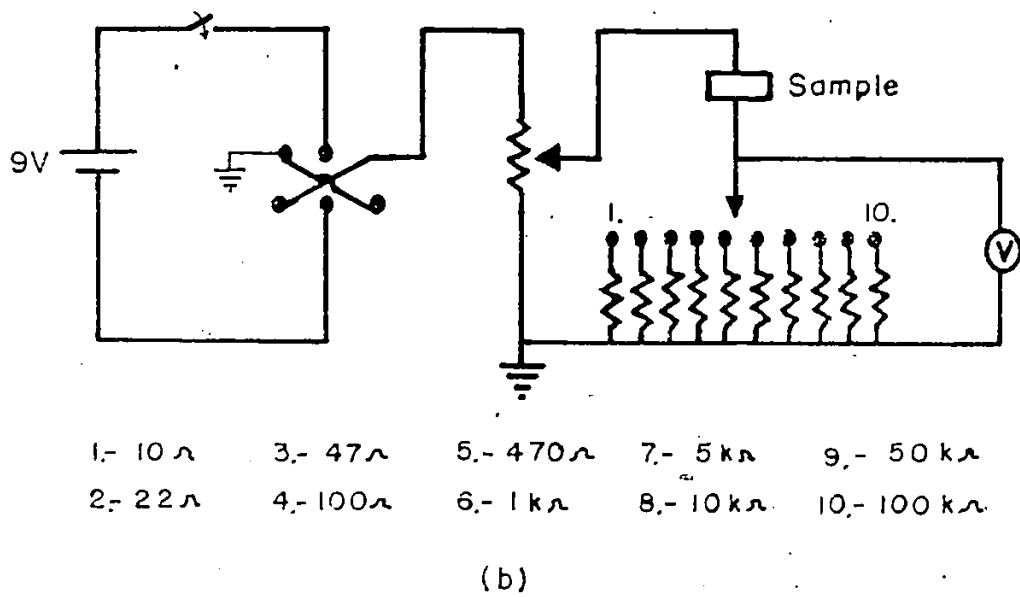
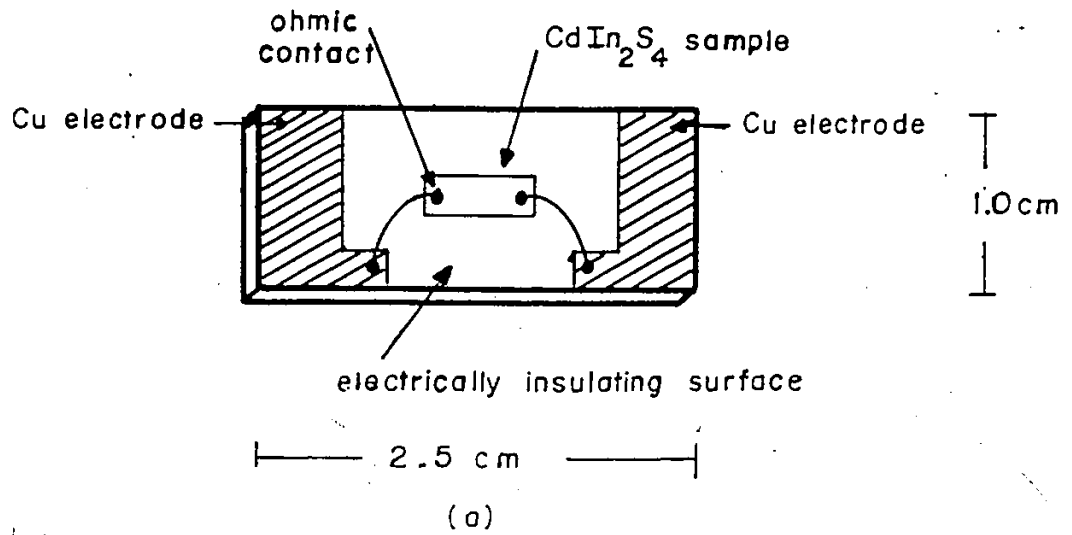


Figure 3.3 a) sample holder ; b) measuring circuit for PC experiment

resistor in series with the sample. The PC response was always normalized for equal incident intensity.

B. High light intensity PC.

A pulse dye laser (pulse width $\Delta t = 2 \times 10^{-6}$ sec) was used as a source of excitation providing intensities of up to 10^{11} W/m² ($\lambda = 600$ nm) at a repetition rate of 10 pulses per second (pps). Details on the pulse dye laser will be given in the next section. The change in conductivity of the sample (or the photocurrent pulse) was detected by measuring the voltage drop across a load resistor, R_s , in series with the sample, using the same circuit as in the low intensity regime (see figure 3.3b). The load resistor was always less than one percent of the sample resistance, R_{sample} , even under the most intense illumination ($R_s \ll R_{\text{sample}}$). With this condition satisfied, circuit loading effects were eliminated; i.e., the signal recorded was directly proportional to the photoconductivity response. Figure 3.4 shows the experimental apparatus for the high intensity measurements. A focusing lens (focal length of 37 cm) was introduced between the pulse laser and the sample to obtain a spot size less than 1 mm in diameter. The intensity of the beam was varied either by inserting calibrated neutral density filters, capable of withstanding high intensity light, in front of the sample or by moving the lens to get a different spot size. With the set of filters used, the excitation density

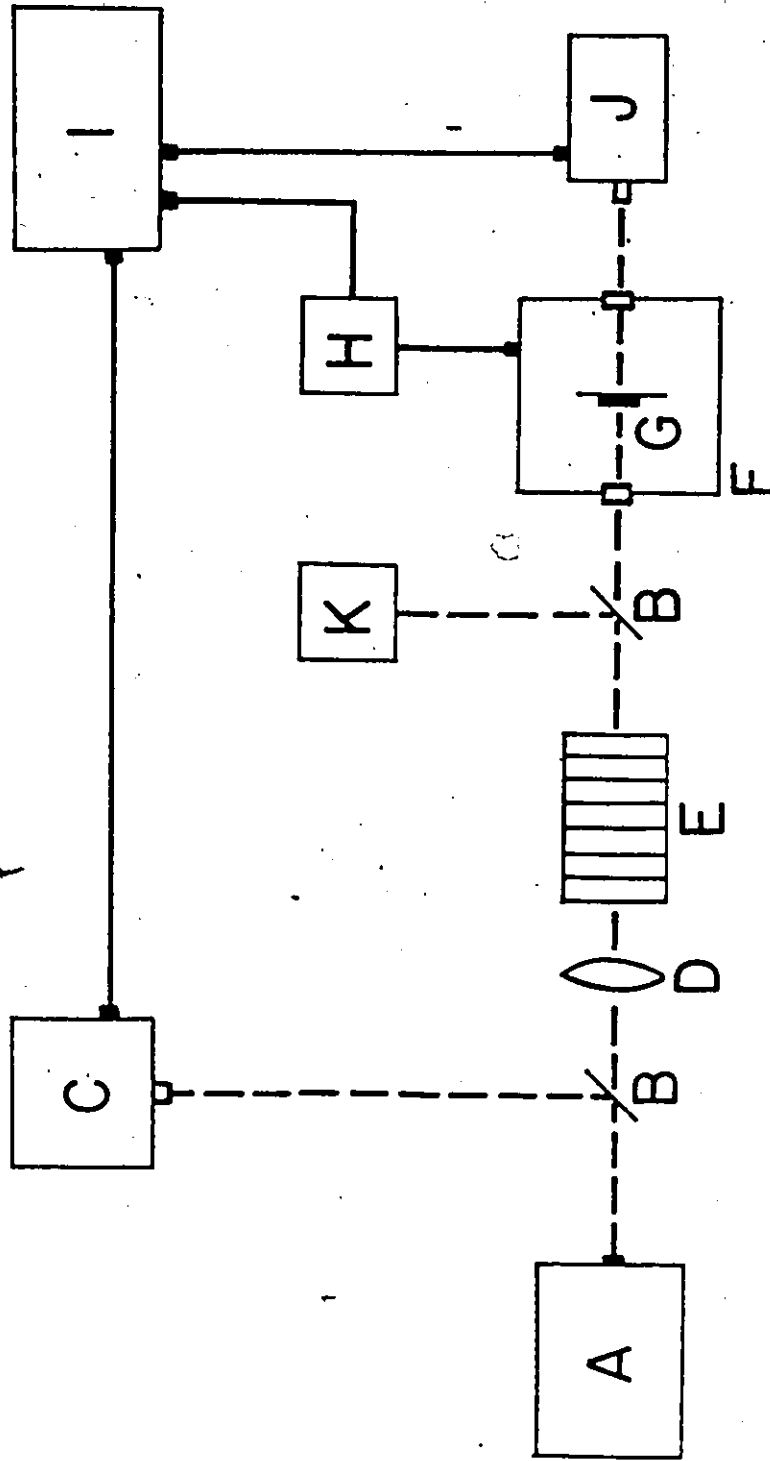


Figure 3.4 Experimental apparatus for the high intensity measurements

- A) Pulse dye laser; B) Beam splitter; C) Optical trigger; D) Lens;
- E) Calibrated neutral filters; F) Optical cryostat; G) Sample; H) Measuring circuit;
- I) Waveform analyser (Lecroy 3500 SA or Boxcar averager); J) Photomultiplier;
- K) Power meter

could be varied from 10^3 to 10^9 W/m² and the movement of the lens gave us an additional two orders of magnitude, to a maximum intensity of 10^{11} W/m². The filters used were not perfectly neutral; their transmission had a small variation as a function of wavelength. A full calibration of the transmission versus wavelength for the filters was necessary for the calculation of the exact intensity of the laser beam at the surface of the sample. The photocurrent produced by excitation of the sample with laser pulses was recorded either by a boxcar averager or a LeCroy 3500 waveform analyser. When the photocurrent pulse was analysed with the boxcar averager, it was possible to observe only one point of the full transient pulse, which was always chosen to be the maximum of the pulse. The weakness of this recording instrument lies in the fact that the full kinetics of recombination, e.g. the decay of the photoexcited carriers, is not seen. On the other hand, the LeCroy 3500 waveform analyser gave the full time dependence of the signal and hence the rise and decay times of the pulse could also be measured as function of incident intensity. In order to safely assume that the measured pulse rise and decay times are physical effects rather than spurious electronic effects one must estimate the jitter. Jitter is the time discrepancy between the laser pulse and when the instrument measures the laser pulse. In much exaggerated form the observed pulse shape (half width) could be a factor of two wider than the real pulse geometry when averaged over many pulses. An electrical trigger could be taken directly from the CMX-4 but the specifications stated that the laser pulse jitter with respect to this SYNC-OUT was ± 100 ns. Instead an optical trigger was used which was assumed to reduce the jitter. The aperture uncertainty of the LeCroy itself was negligible (± 10 p sec).

The photo currents produced were sampled at a rate of 10^8 times per second with a transient signal averager over 250 scans to increase the signal to noise ratio. Unfortunately, the real time resolution given by the output response to a negligibly short input pulse could not be done because fast optical sources were not available.

C. Optical absorption versus intensity experiments.

The absorption experiment is introduced in the PC section because of the similarity in the detection technique used. The excitation was again in the form of single pulses ($\Delta t = 2 \times 10^{-6}$ sec) in the spectral range from 590 to 620 nm. The exciting radiation was directed to the sample mounted on a pinhole (800 microns in diameter) and placed in a nitrogen cryostat. A set of calibrated neutral density filters was used to vary the excitation density at the sample surface from 10^1 to 10^9 W/m². The transmitted light was recorded using a Hamamatsu R-446 photomultiplier (PM) coupled to a waveform analyser. The typical rise time of the PM is 2.2 nsec and the time resolution around 10 nsec. The operational voltage of the PM was 800 volts. To overcome the possible experimental error due to constant changing of the amplifier gain when a filter was removed, a new technique developed by Radautsan et al.⁽³⁵⁾ was used. Instead of simply removing the filters from the front of the sample to increase the excitation intensity, the filters were transferred to the other side of the sample, just in front of the photomultiplier. In this way, the total number of filters in front of the PM remained constant although the light intensity at the crystal

surface could be changed. In this way the variation of the signal detected by the PM could be attributed solely to the variation of the coefficient of absorption of the crystal. In other words, a decrease in the coefficient of absorption of the crystal leads to an increase in transmitted light and thus a higher signal will be recorded by the PM. This technique assured that the non-linearity due to the PM response was negligible since the variation of intensity at the PM was extremely small. Some experimental problems were encountered in this experiment and these will be discussed in chapter 4.

3.4 Laser CMX-4 description.

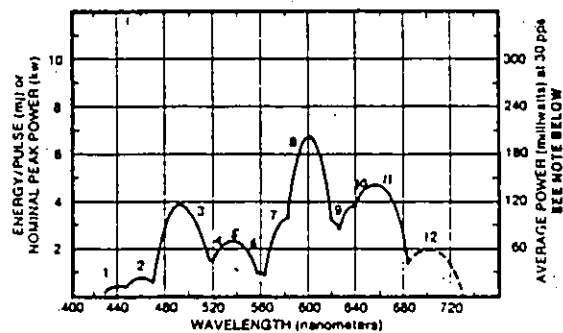
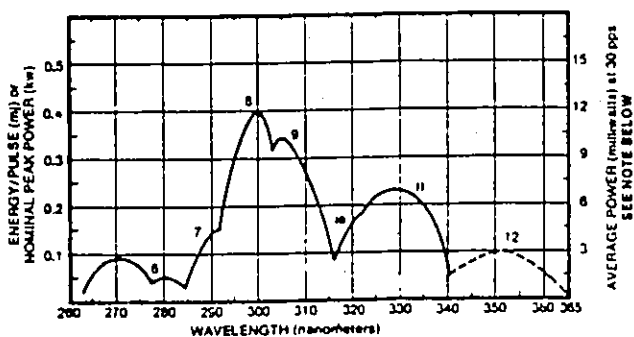
To the author's knowledge, no other formal research work has been done with the CMX-4 laser, here at the University of Ottawa. Hopefully, the following description will provide a guide for other students in the use of this piece of equipment. The Chromatix model CMX-4 flashlamp pumped dyes laser provides continuously tunable radiation in the visible portion of the spectrum (tuning range between 435 to 730 nm). The horizontally polarized beam diameter is approximately 3 mm at the output mirror and the beam divergence is less than 1 milliradian at 5 pps. The pulse repetition rate can be set to 5, 10, 15, 20 or 30 pps, and the pulse amplitude stability is $\pm 10\%$ at 5 pps. To obtain different wavelength ranges, laser dye which are colored organic compounds dissolved in a suitable solvent, are used. In the CMX-4, optical pumping of the dye molecules is accomplished by radiation from a Xenon flashlamp which must be changed every 10^6 pulses. Table 3.1 taken from the instruction manual shows the different possible dyes which can be used with this laser.

For this work, only two dyes were used: Rhodamine 6G and Coumarin 102. The instruction manual gives a good description of dye preparation. The Rhodamines are, in general, very strong dye and can last for approximately 300,000 pulses, in comparison with Coumarin 102 which lasts no longer than 100,000 pulses. It should be noted that, in contradiction to the manual, the dye #9 (Rhodamine 6G with 4% Ammonyx LO) gave 20% more power than the other Rhodamine 6G (dye #8), so that dye #9 was usually used in the 580-630 nm region. Moreover, at the beginning of the dye's life, the power could easily reach two times the average power indicated in the manual but after several thousand pulses the average power drops rapidly to a plateau at a value of approximately half the original power. In the case of Rhodamine, this plateau at half power last for about 250,000 pulses. Finally, an important characteristic to notice is that the pulse shape, as measured by the PM, is different for the two dyes, as will be seen later. Futhermore, with continued use of the dyes and the electrical components (eg. spark plug), the pulse shape may change. The biggest change being the increase of laser pulse halfwidth. Unfortunately, it was not possible to record the pulse shape after each experiment so an uncertainty of $\pm 10\%$ will be attributed on the recorded value.

I would like to end this section by mentioning that this laser requires a lot of attention and maintenance for the achievement of good results. The manual provides the necessary information on dye preparation and laser maintenance.

Table 3.1 DYE RANGES AND POWER CURVES

Curve	Dye	Tuning Range (nm)	Peak Gain Wavelength (nm)
1	Coumarin 120	435-455	442
2	Coumarin 2	445-482	460
3	Coumarin 102	476-518	490
4	Coumarin 30	493-540	512
5	Coumarin 522	518-567	534
6	Sodium Fluorescein	542-577	558
7	Rhodamine 575 (1:1 water/ Methanol)	566-610	590
8	Rhodamine 6G (1:1 water/ Methanol)	577-625	598
9	Rhodamine 6G (4% Ammonyx LO)	585-633	610
10	Kiton Red S	622-665	642
11	Rhodamine 640	635-700	667
12	Oxazine 170	675-730	705



NOTE: Dashed curves are for peak powers and energy per pulse only, not average power.

3.5 Photoluminescence experiment.

A. Photoluminescence emission spectra*

For the PL emission spectra, a fixed wavelength is used as an excitation source and the radiation coming off the crystal at different wavelengths is recorded. The intrinsic excitation experiments were done at NRC. The samples were placed in a variable temperature (4.2 - 300 K) Oxford Instrument optical cryostat. The luminescence, induced by a line of CW argon ion laser, was analyzed by a Spex monochromator and detected by a S-1 photomultiplier coupled to a Datamate analyser. The resolution of the system was 0.5 nm. Different laser excitation powers ranging from 5 mW to 100 mW were used and the wavelength used was 457.9 nm in order to obtain interband excitation. The exciting photon density was of the order of 10^{22} photons/m²-sec at 10 mW and 457.9 nm. A high pass optical filter was inserted between the sample and the spectrometer in order to cut the reflection of the laser beam from the sample, and to eliminate the stray light coming in the spectrometer. The filter cuts off everything below 500 nm but lets pass higher wavelengths, in this case, the luminescence. The geometry of this experiment was the standard 45° set up, in which the laser beam hits the sample at 45° and the reflected beam is focused into the spectrometer. All the PL emission spectra were normalized for the PM and spectrometer response.

Extrinsic excitation luminescence spectra were acquired at the University of Ottawa. A He-Ne laser and a mercury lamp with appropriate high pass filters were used as exciting sources. In this case, a McPherson grating monochromator was used as the dispersive element and the luminescence was detected by a GaAs - photomultiplier coupled to a lock-in

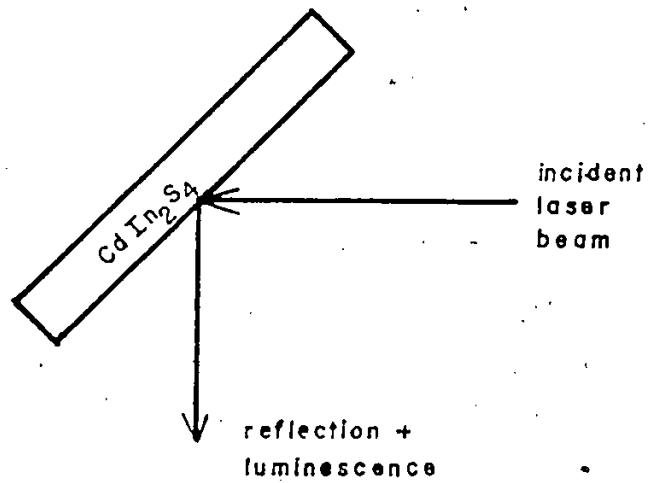
* part of the research done at the National Research Council of Canada, Ottawa, Ontario.

amplifier. Here again the emission spectra were normalized in order to take into account the grating efficiency and PM response.

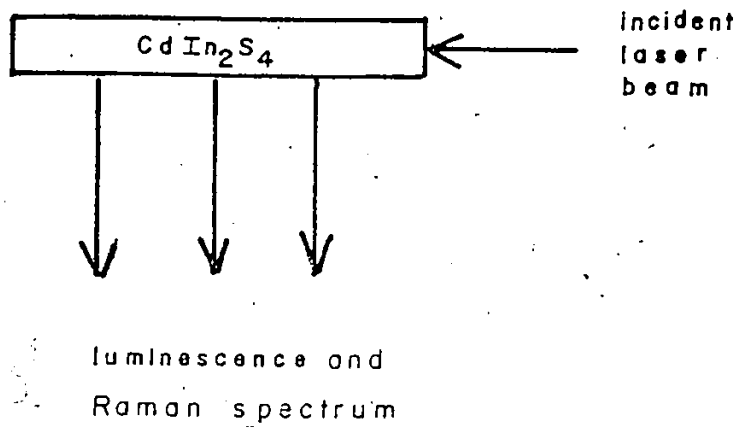
B. Photoluminescence versus intensity and PL transient experiment.

A pulse dye laser (CMX-4) operating at 490 nm and 600 nm and providing high intensity light was used as an excitation source. The PL versus intensity measurements were done at 100 and 300 K. The luminescence was analyzed by a McPherson grating monochromator coupled to a Hamamatsu photomultiplier and recorded by a waveform analyser and the luminescence signal was averaged over 250 pulses. For these experiments, only one wavelength of the luminescence spectra was analyzed. The spectrometer was always set to observe the maximum of the luminescence band. The maximum slit widths of the spectrometer were used, giving a resolution of 2 nm. The excitation intensity was varied by means of neutral density filters. The geometry used for the two exciting wavelengths (490 nm and 600 nm) was different since, in the former case, band to band transition was achieved (all the light was absorbed near the surface of the sample) and, in the latter, the light was absorbed in the bulk. To maximize the luminescence intensity, the standard 45° geometry was used for the interband excitation and the 90° geometry for the extrinsic excitation (figure 3.5). The reason for the choice of the latter geometry is simple. Since the coefficient of absorption in the extrinsic spectral region is very low, a thicker sample would provide more absorption and therefore more luminescence. (No Raman line or band was observed in this spectral region studied).

In summary, a number of experimental techniques, including PC, PL and optical absorption at high light intensities were used to provide novel information on the optical properties of CdIn_2S_4 samples. The information derived from these techniques and the application of this information to the understanding of this type of alloy will be discussed in the next chapter.



(a)



(b)

Figure 3.5 Photoluminescence geometry a) 45° and b) 90°

IV RESULTS AND DISCUSSION

As previously mentioned, photoconductivity and photoluminescence spectra at different temperatures were acquired in order to characterize the CdIn_2S_4 crystals. From these results, the energies of the transitions involved in the excitation and recombination processes or the position of the impurity levels inside the gap can be found. The Lux-Ampère experiments and measurements of rise and decay times of the PC transients were performed over twelve orders of magnitude of exciting light. Absorption in the extrinsic region of CdIn_2S_4 was measured as a function of light intensity. Finally photoluminescence intensity versus intensity of excitation, as well as PL transients at 100 K and 300 K will be discussed.

4.1 Photoluminescence spectra

The photoluminescence experiments were performed in order to investigate the radiative recombination processes; one of the possible processes by which carriers decay. The luminescence spectra were also used to determine whether the samples studied follow the reported band diagram proposed for CdIn_2S_4 ⁽¹³⁾ (see Figure 2.2).

As explained in section 3.5, the PL spectra of CdIn_2S_4 was measured in the temperature range 4.2 - 300 K and excited with the 457.9 nm line of

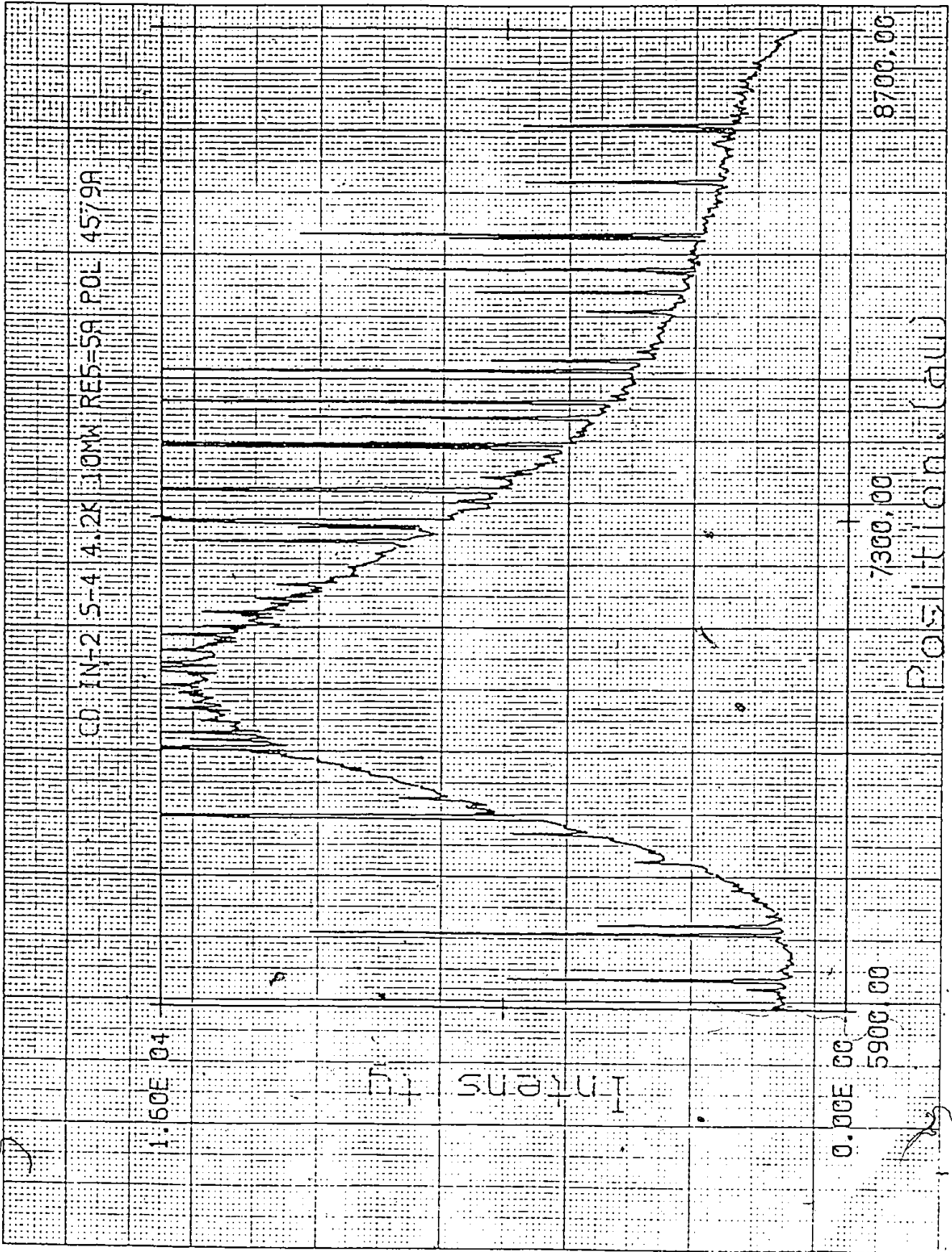
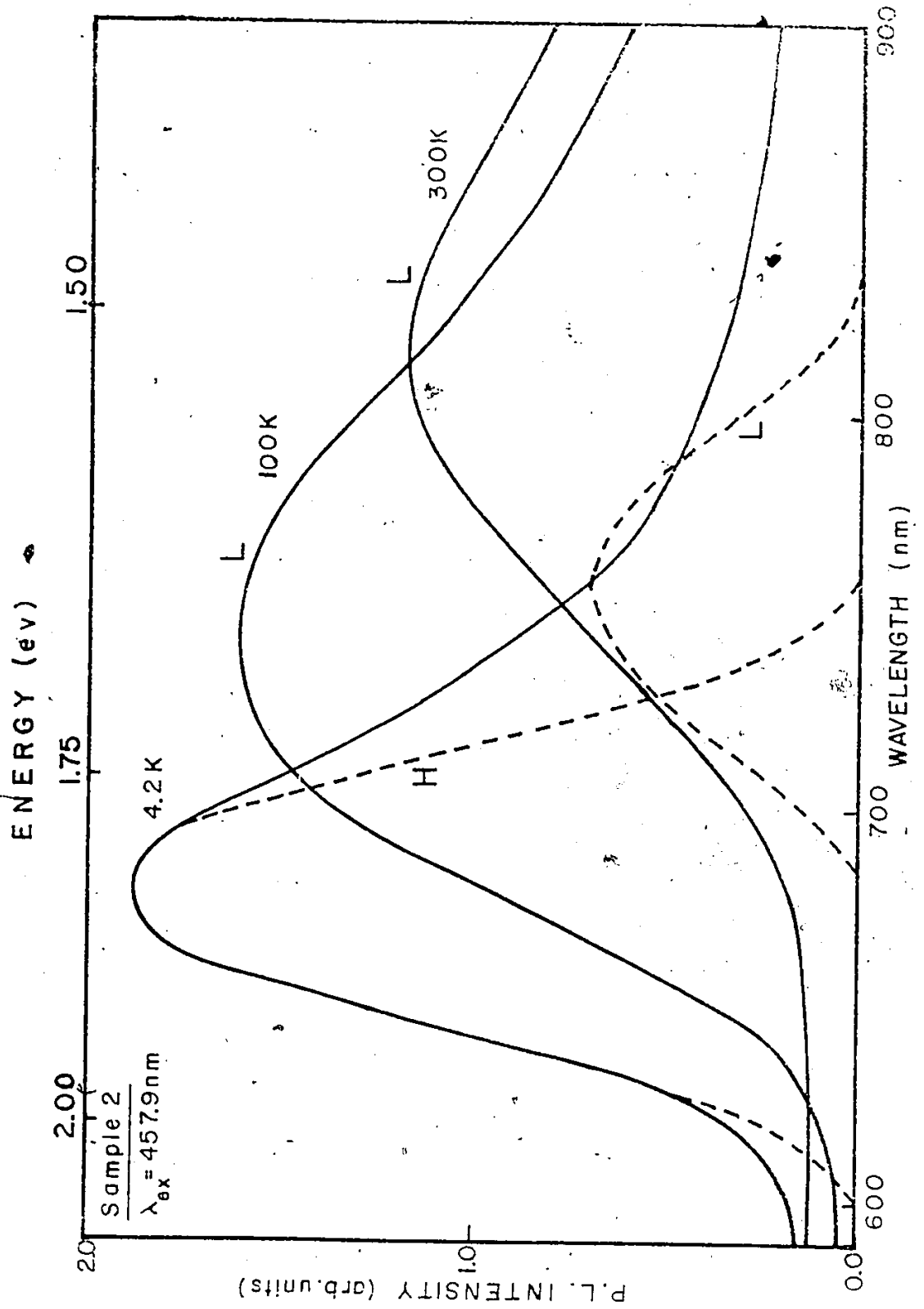


Figure 4.1a Photoluminescence emission spectra of CdIn₂S₄ at 4.2K (raw data)

an argon ion laser. This wavelength was used in order to obtain interband excitation. Figure 4.1a shows the actual PL raw data obtained by the system. The sharp line in the spectra correspond to laser plasma lines and are of no interest here. Representative PL spectra, obtained at 4.2, 100 and 300 K, are shown in figure 4.1b. At room temperature, the luminescence spectrum is composed of a single band of Gaussian shape centered at 1.52 eV (815 nm) with a halfwidth of 0.34 eV. For temperatures lower than 100 K, the luminescence spectrum displays a complex structure: a second narrower luminescence band appears at higher energies; the ratio of the intensities of the high energy band (called the H-band) and the low energy band (called the L-band) increases with decreasing temperature. The low temperature spectra have been numerically decomposed into two Gaussian components. The agreement between the experimental spectra and the sum of the two components is on the order of the experimental errors. At $T = 4.2$ K, the L-band maximum is located at 1.63 eV (760 nm) and its halfwidth is approximately 0.20 eV; the energy of the maximum and the halfwidth of the H-band are 1.83 (677 nm) and 0.20 eV respectively. The spectra obtained are therefore in agreement with most of the published results on the luminescence of CdIn_2S_4 single crystals grown by the chemical transport method (12, 13). The luminescence spectra of different samples are very similar, the only difference between them being the relative intensity of the emission bands which is not of interest in the present section.

The luminescence spectra were also acquired with different excitation sources including a He-Ne laser (632.8 nm; 1.95 eV), a mercury lamp with appropriate high pass filters and a pulse dye laser (600 nm; 2.10 eV). Interesting behaviour was observed when the excitation energy was below the band gap value (2.45 eV). For excitation energies of 2.10 and 1.95 eV,

Figure 4.1b Photoluminescence spectra at 300, 100 K and 4.2 K



only the L-luminescence band was seen and for excitation energies higher than 2.35 eV, both the L and H bands were observed.

In our scheme, we called E the acceptor level and T the trap distribution (Figure 2.2). It has been proposed⁽¹³⁾ that the L luminescence band is due to the electron transition 3 from the trap distribution T to the acceptor level E. This proposal can be justified by the high density of the E and T centers, and can also give an account of two features of the L band; its relatively large halfwidth and the anomalous temperature dependence of the halfwidth (figure 4 of reference 13). The halfwidth of the L-band is nearly constant between RT and 250 K, broadens when the temperature decreases from 250 to 150 K and again becomes constant at lower temperatures. In comparison, the halfwidth of the H-band displays the usual behaviour, being temperature independent at low temperature and increasing monotonically at higher temperatures.

As explained earlier, when the sample was excited at 2.10 eV at 100 K, only the L luminescence band was excited; however at the same energy, a strong photoconductivity band was observed (section 4.2) and was attributed to transition 2 from the relaxed acceptor level E, to the conduction band.

The higher excitation energy (2.35 eV at 100 K) excites both the L and H luminescence bands. At this energy at low temperatures, a negligible photoconductivity was observed. The proposed transition of this process is from the valence band to an excited donor level V^* . The donor level V^* can relax and the electron can make the radiative transition from the V level to the valence band at 1.85 eV, giving rise to the luminescence H-band.

Alternatively, the electron can tunnel to the trap and recombine radiatively with a hole trapped in the E-center. The tunneling, $V \rightarrow T$, is promoted by the high density of trapping levels with energies of the order of the energy of the V level.

In summary, when the excitation provides band to band transitions, both L and H luminescence bands are seen at temperatures lower than 100 K, and for temperatures higher than this, only the L band is seen. The explanation for this phenomena is that the Fermi level moves with temperature. When $T < 100$ K, the Fermi level lies above the V-centers so that all of the centers are occupied and the transition V to conduction band can be observed. Furthermore, optically excited electrons can be trapped by the T level and decay via transition 3, so that both processes of recombination are observed. As the temperature is increased, the Fermi level decreases and when $T > 100$ K, the Fermi level lies below the V-centers so that each donor is unoccupied by electrons. Now photoexcited electrons can be captured by both T and V-centers. Due to the high density of trapping levels T and their high capture cross section combined with the fact that the V-centers have a small capture cross section for free electrons,⁽¹³⁾ the most probably process of recombination is by the traps T and transition 3 giving rise to the L-luminescence band only. When the excitation energy is 2.10 eV and the temperature is higher than 100 K, the electrons are excited from the E level to the conduction band, where they are trapped and make radiative transitions from the T-levels to the excited E-levels, producing the L-luminescence band. At an excitation energy of 2.35 eV, the electrons are excited from the valence band to the V^* -level. Some of the electrons return to the ground state of the V-level then radiate energy by the transition V to valence band producing the H-luminescence band and others tunnel through the traps and decay via

transition 3 producing the L-band. In conclusion, the important thing to remember is that at temperature higher than 100 K, the V -centers play no role in the recombination processes at any excitation energies studied.

4.2 Photoconductivity spectra.

As was the case with the PL emission spectra, the PC spectra were acquired for the characterization of the samples. In figures 4.2 to 4.4 the PC spectra of CdIn_2S_4 at RT and 100 K are reported for three different samples. The spectra have been normalized for equal incident intensity and the chopping frequency used was 44 Hz. It is important to remember that the PC spectrum does not necessarily follow the optical absorption spectrum, since PC depends on both the optical absorption and the lifetime of the photogenerated carriers in the crystal. The vertical scale is in arbitrary units, since only the shape of the spectra is of interest here. Furthermore, the exact shape of the spectra, and the relative intensities of the peaks depend upon the preparation conditions under which the sample was grown and therefore varies from sample to sample.

For the three different crystals (sample 1-3) at both temperatures, the spectra show two peaks. Table 4.1 (a) summarizes these results by giving the position of the peaks for the three samples at 100 K and 300 K. Table 4.1 (b) shows the resistance of the samples when the electrical (ohmic) contacts are 1 mm from each other at RT and 100 K. R_{dark}

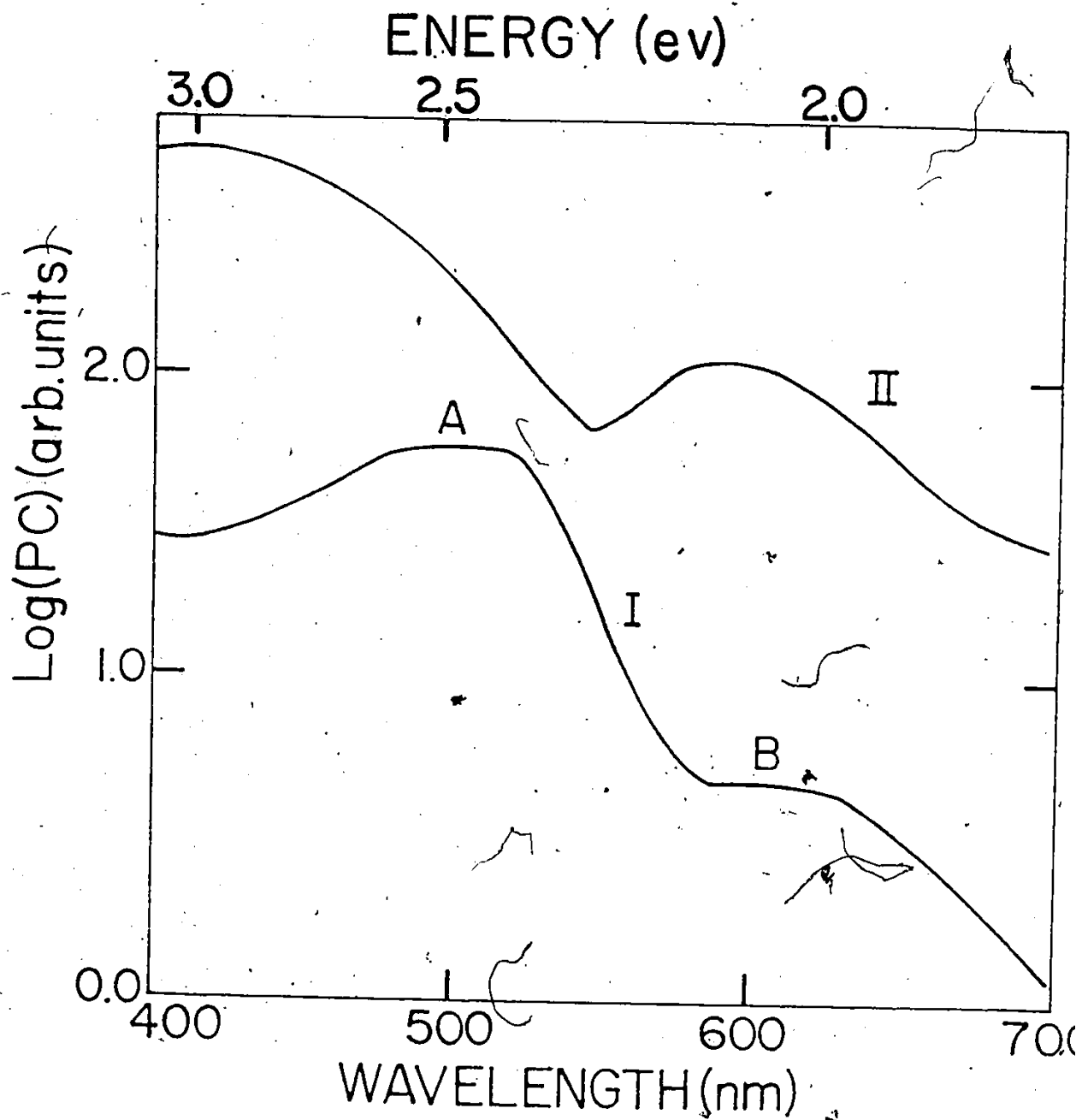


Figure 4.2 PC spectra of Sample 1 at Rt (I) and 100 K (II)

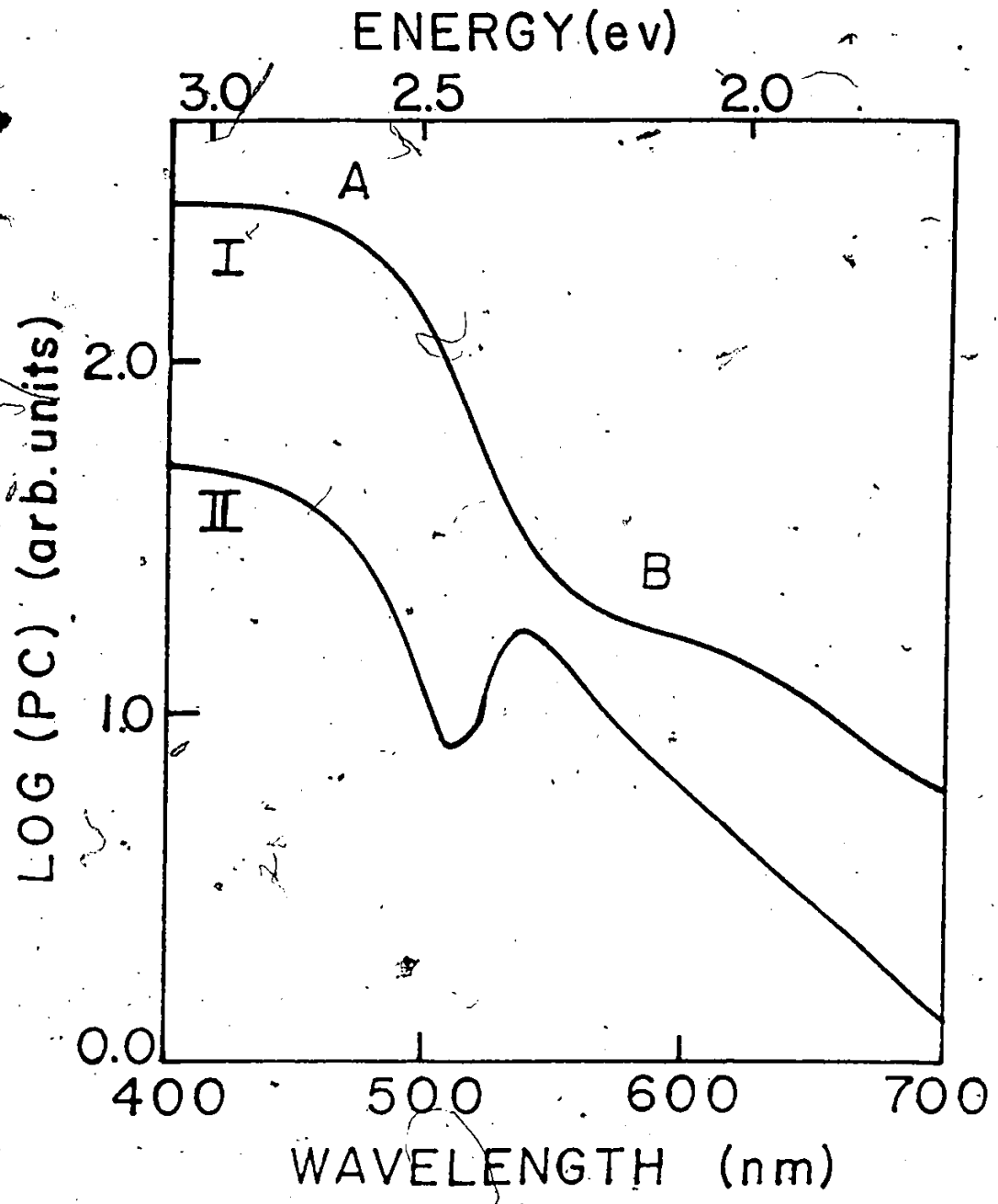


Figure 4.3 PC spectra of Sample 2 at RT (I) and 100 K (II)

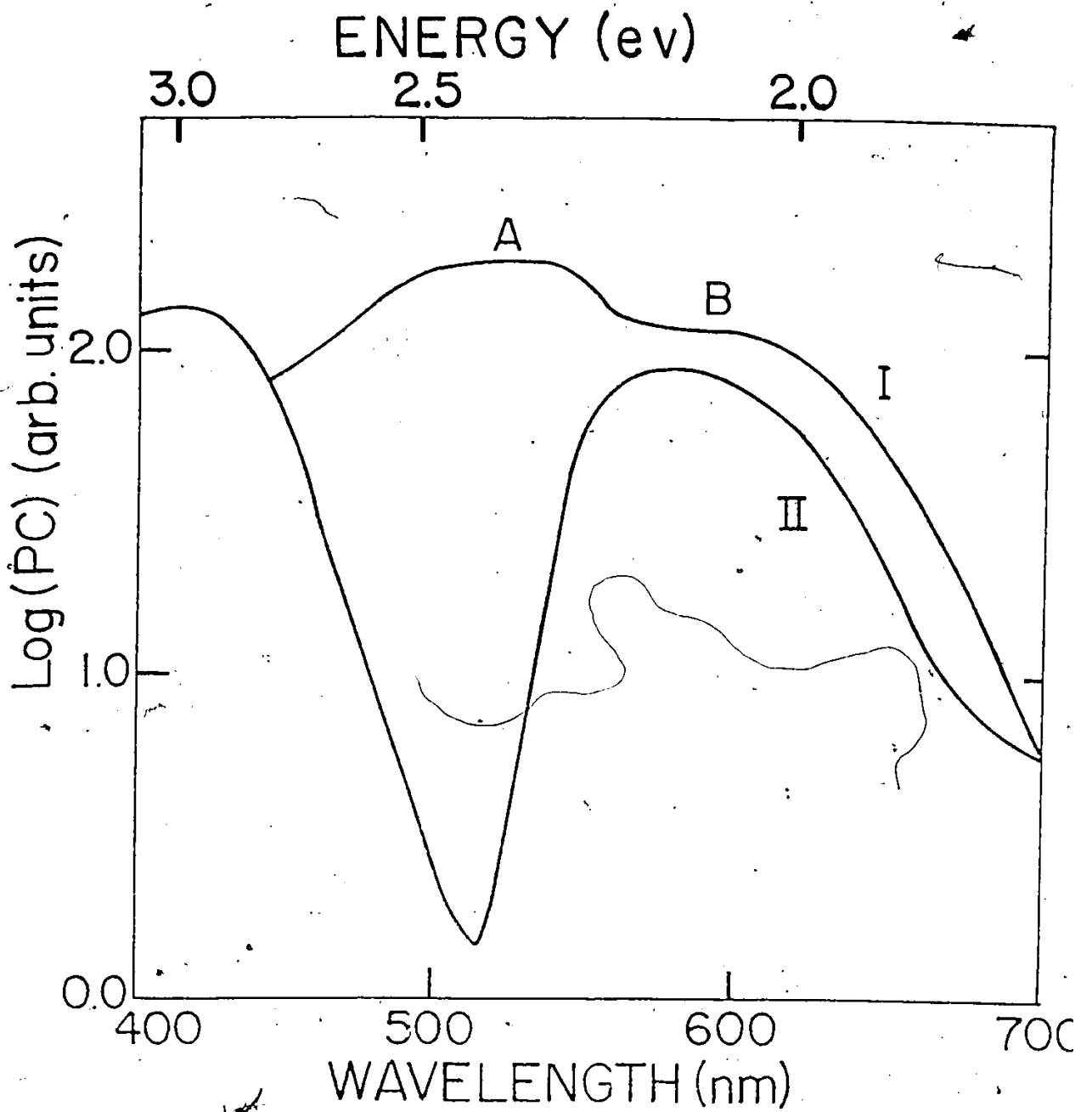


Figure 4.4 PC spectra of Sample 3 at RT (I) and 100 K (II)

Table 4.1

a) Position of the peaks in the PC spectra

	position of the peak		position of the peak	
	300 K		100 K	
	peak A (nm)	peak B (nm)	peak A (nm)	peak B (nm)
Sample 1	500	600	425	585
Sample 2	450	600	425	550
Sample 3	510	600	425	585

b) Photo-electronic properties of CdIn_2S_4

	300 K		100 K	
	$R_{\text{dark}} (\Omega)$	$R_{\text{WL}} (\Omega)$	$R_{\text{dark}} (\Omega)$	$R_{\text{WL}} (\Omega)$
Sample 1	8.2×10^4	4.1×10^4	3.0×10^6	4.5×10^5
Sample 2	4×10^7	8×10^6	1.0×10^8	1.0×10^6
Sample 3	7.5×10^4	3.7×10^4	2.2×10^6	3.3×10^5

corresponds to the dark resistance of the samples and R_{WL} to the resistance of the crystal when it is illuminated by a 40 Watt quartz-iodine lamp at a distance of 30 cm. Samples 1 and 3 have approximately the same resistivity, whereas sample 2 has a higher impedance. Differences can also be seen in the position of the peaks in the PC spectra: samples 1 and 3 have their peaks at the same energies but the peaks in sample 2 are shifted to lower wavelength. Abdullaev et al.⁽¹⁸⁾ measured the PC on a large number of single crystals prepared by the chemical transport method and suggested that a deviation from the stoichiometric concentration of sulfur made some changes in the structure of the energy band. The data shows that the resistivity of the crystals is directly related to the sulfur content of the sample and can vary considerably from sample to sample. We can, therefore, safely assume that the samples used have different degrees of sulfur content (sample 2 has a lower concentration of sulfur than sample 1 and 3).

Peak A, of the PC spectra, can be attributed from previous studies^(8, 18) to band-to-band transitions (transition 1 in figure 2.2). Peak B, at 2.1 eV, owing to the very low absorption coefficient in this spectral region, can be regarded as a volume effect; its strong enhancement at low temperatures involves the contribution of a localized state. The origin of peak B was suggested by Abdullaev et al.⁽¹⁸⁾ who found that this peak is prominent in non-stoichiometric sulfur-excess samples. This peak, observed in the same position in luminescence excitation spectra, is assigned, in agreement with Czaja and Krausbauer⁽¹⁵⁾, to the electron transition from an ionized acceptor level E to the conduction band

(transition 2 in figure 2.2). Photoluminescence emission spectra reported by Grilli et al⁽¹³⁾ indicate that electron relaxation occurs via trap states T and transition 3 in figure 2.2.

Finally, the PC spectra were also recorded at different chopping frequencies varying from 22 Hz to 710 Hz. No change in the position or relative intensities of the peaks were noticed at either temperatures, providing that both transition processes 1 and 2 are faster than 1 msec, i.e. a steady-state condition was always achieved over the range of chopping frequencies studied. Now that the excitation and recombination processes are known at the two temperatures for the different crystals, let us look at the change of the PC response with the intensity of excitation.

4.3 Photoconductivity versus intensity (low light).

It should be emphasized at this point that a concept fundamental to the interpretation of PC presented in this thesis is that in CdIn_2S_4 , extrinsic excitation ($h\nu < E_g$) produces free electrons while holes play an insignificant role in the extrinsic PC process. This assumption is based on the fact that all previous research indicates n-type PC⁽⁸⁾.

PC versus intensity measurements (at low light intensities) were performed for the three samples in the energy region of peak A and peak B at RT and 100 K. The Bausch and Lomb monochromator was used as a source and some Balzers calibrated neutral density filters were used to vary the incident intensity. All the experiments were done at a chopping frequency

Table 4.2 Effects of increasing light intensity on PC response.

Sample	λ_{exc} (nm)	I_o^a (W/m ²)	Slope ^b	
			300 K	100 K
1	500	1.70	1.00	--- ^c
	600	2.54	0.95	--- ^c
	450	0.95	--- ^c	0.70
	585	2.51	--- ^c	0.85
2	450	0.95	0.80	--- ^c
	600	2.54	0.90	--- ^c
	425	0.65	--- ^c	0.80
	550	2.33	--- ^c	1.00

a. maximum intensity

b. taken from fig 4.5 - 4.6

An uncertainty of ± 0.02 is attributed on the values of the slopes. This value was obtained by statistical means using the spread about the line assuming no uncertainty on individual points. (ref. P.R. Bevington "Data reduction and error analysis for the physical sciences").

c. no measurement.

of 44 Hz. Figure 4.5a and 4.5b show a log-log plot of the PC response as a function of light intensity for sample 1, at RT and 100 K respectively for two wavelengths of excitation corresponding to optical transitions of peaks A and B. Figure 4.6 shows the same dependence for sample 2.

It should be noted that the light intensity on the graphs is expressed in units of optical density (O.D.) which is defined in the following way:

$$\text{O.D.} = -\log_{10} I/I_0$$

where I_0 is the maximum intensity one can achieve in the absence of filters. Then the intensity at the surface of the sample is given simply as

$$I = I_0 10^{-\text{O.D.}}$$

The same experiments were done on sample 3 with results comparable to sample 1, so sample 3 will not be considered in the present section. It should be emphasized that when the excitation was done from a chopped light source the steady-state condition was achieved since the process of decay was of the order of 10^{-5} sec (as will be discussed in the next section) and the chopping frequency was 44 Hz giving rise to a period of excitation of 2×10^{-2} sec.

Table 4.2 summarizes the results obtained for samples 1 and 2 at the two temperatures studied. Note that all the slopes are either linear or sublinear ($\frac{1}{2} < \alpha < 1$). There exists a single physical picture to account for exponents less than unity derived from the distribution of N_c states. The model, explained in section 2.2, proposes that as the light intensity is increased, more and more of the N_c states are converted from trapping to

Figure 4.5 PC versus intensity (low light) for Sample 1 a) RT and b) 100 K

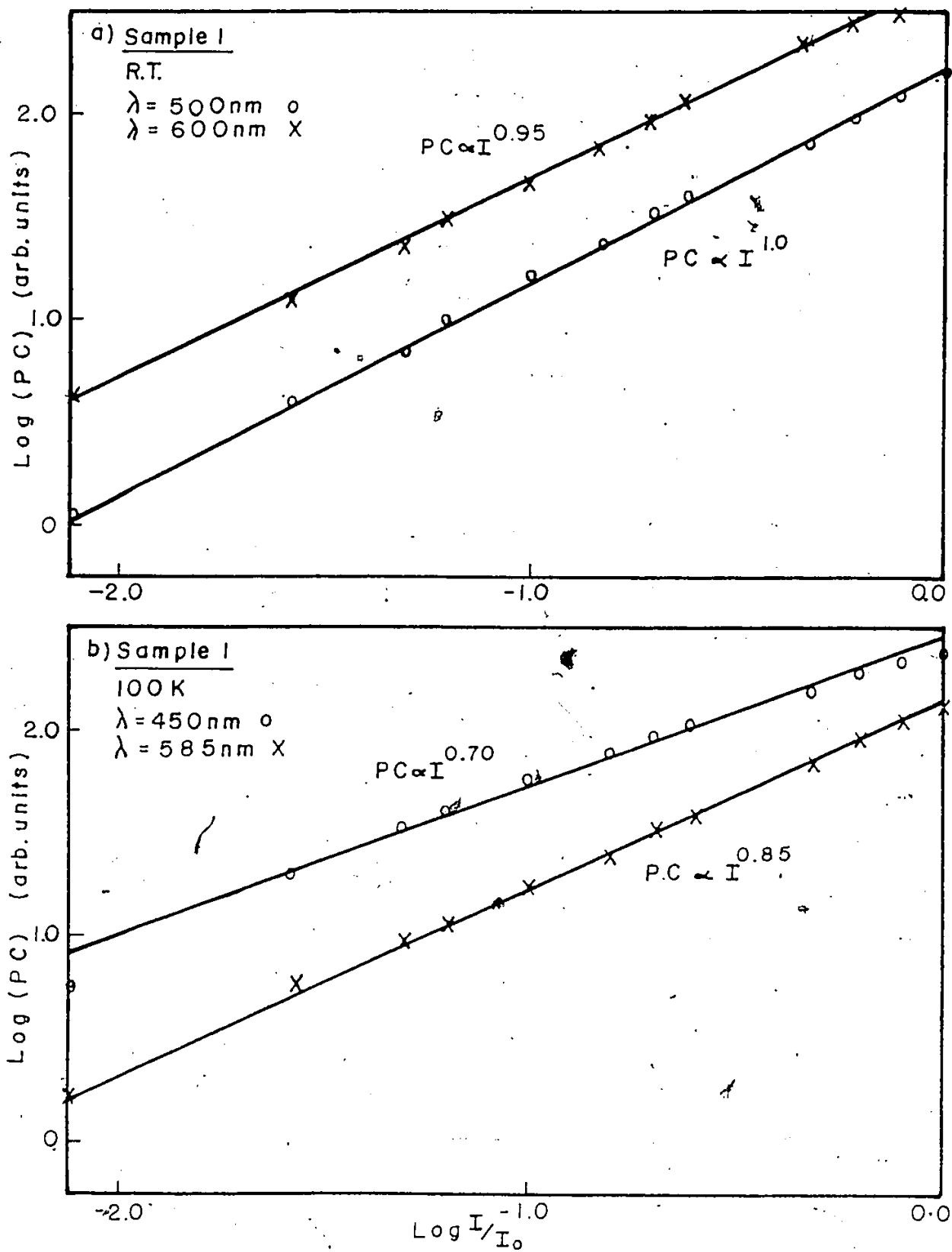
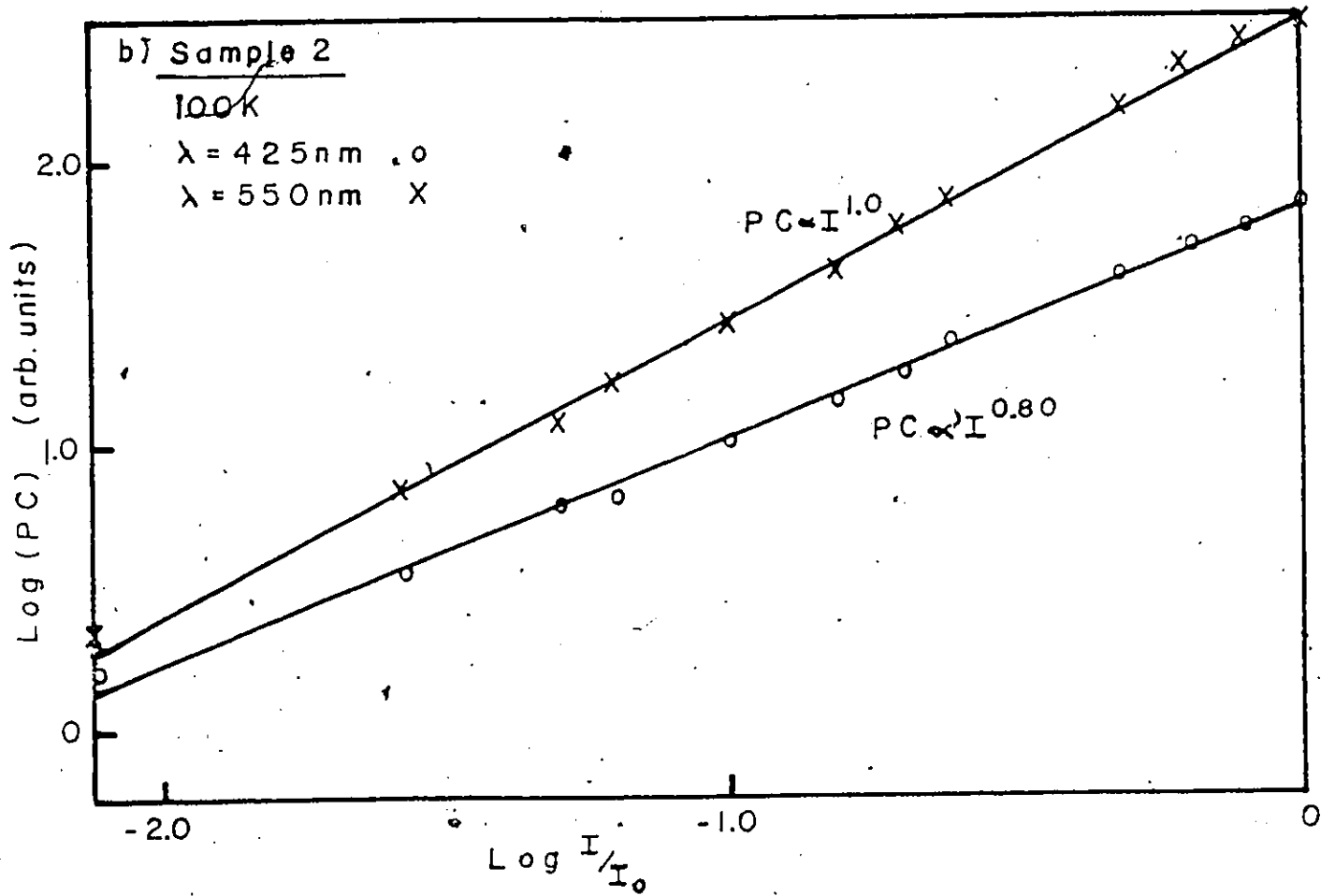
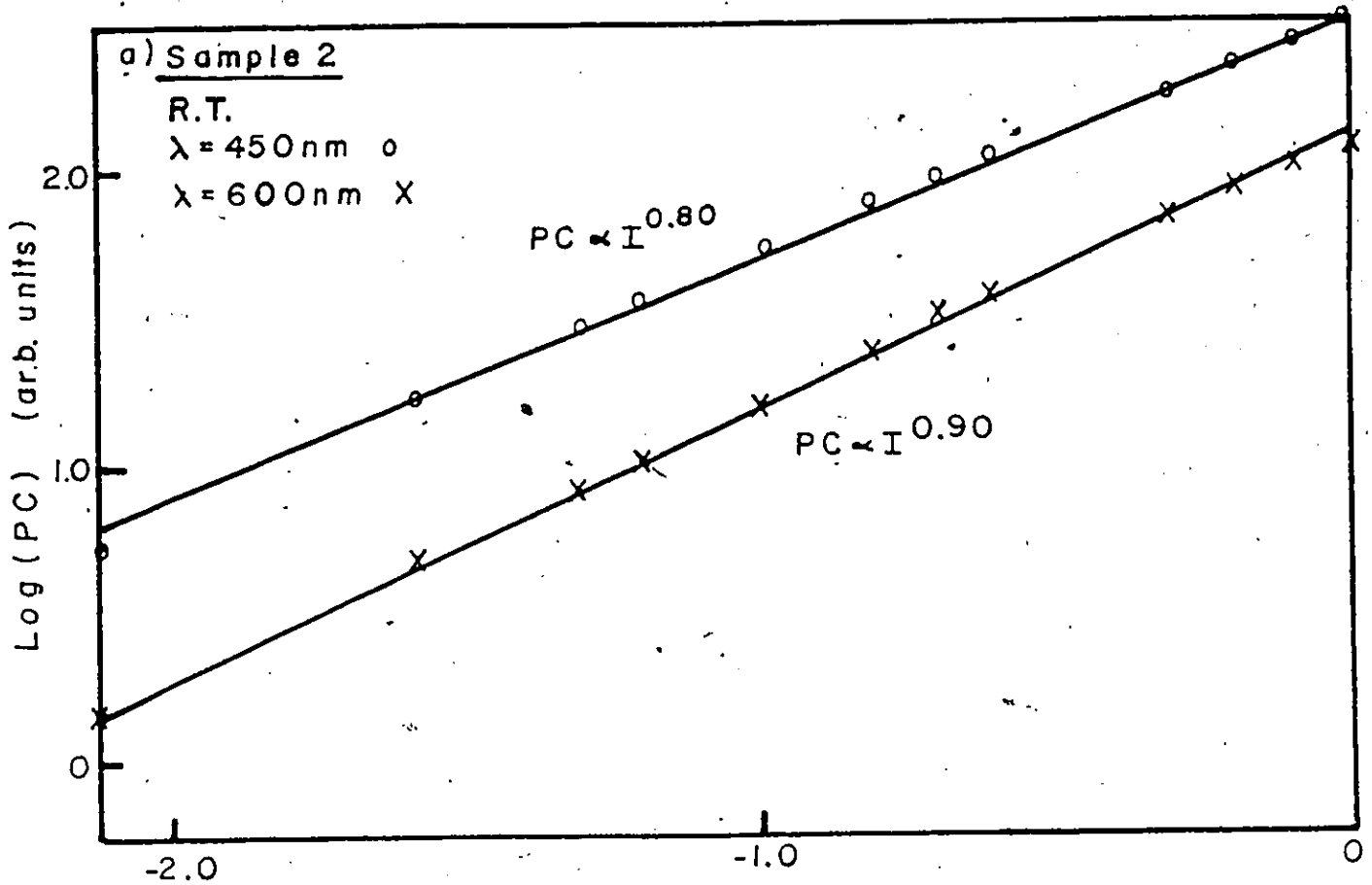


Figure 4.6 PC versus intensity (low light) for Sample 2 a) RT and b) 100 K



recombination states. This conversion takes place as the steady-state Fermi level E_{fn} sweeps through the N_t states towards the conduction band. As p_r , the density of recombination states for electrons, increases, the electron lifetime decreases. This model is valid for both electrons excited from the valence band to the conduction band giving rise to free pairs (peak A) and for electrons excited from the recombination states to the conduction band (peak B). Thus, the sublinear behaviour of the log (PC) versus log (intensity) plot implies a decrease in the carrier lifetime with intensity, whereas a linear dependence implies no change in lifetime. As for the actual values of the slopes at both temperatures for the 2 samples, they are closely related to the purity of the crystal and thus the extrinsic disorder on which we had no control. For example, different samples may have a different distribution of traps in energy which could have a direct effect on the value of the slope. The change in lifetime of excited carriers with intensity will be discussed in more detail in the next section.

4.4 Photoconductivity versus intensity and PC transient kinetics. (high light intensity).

A. PC transient kinetics.

With peak laser pulse intensities one hundred million times greater than the intensities used in the chopped excitation modes, it is likely that the kinetics are very different. PC transients, using the pulse laser as a source of excitation, were measured for two reasons. The first was to

see if the steady state condition was achieved using pulsed excitation and the second to detect if a variation of the decay time of photoexcited carriers with intensity and temperature could be seen. These experiments provide additional information about the kinetics of recombinations, as will be seen later. In the present analysis, the decay time of photoexcited carriers will be given by the time required to go from the maximum of the PC transient pulse to 60% of the same maximum. Using a laser pulse width of $\Delta t = 2 \times 10^{-6}$ sec as an excitation source, it is expected that the response time be now of the order of μ sec rather than milliseconds as was the case in the low intensity regime.

In the present analysis, the results of section 4.1 and 4.2 will be taken into consideration. Recall (section 4.1) that the V-level plays no role in the recombination process in the temperature range studied. Furthermore, it will be demonstrated in section 4.6 that the ionized E-center has a large capture cross section for free holes whereas the non-ionized E-center has a small capture cross section for free electrons. Also, the trapping levels (T) will be shown to be very efficient in the capture of free electrons. Finally, as will be demonstrated from the PL transient kinetics experiment (section 4.6), free electrons can also recombine via a nonradiative process. For the present investigation, only sample 3 will be considered in detail, the other two samples giving the same general dependence.

Figures 4.7 and 4.8 show the PC transients for sample 3 at RT and 100 K in the optical region of peak A (490 nm) and peak B (600 nm) respectively. Figure 4.8c shows an example of the PC transient raw data printed from the LeCroy 3500. In this case a dwell time of 20 nsec was used.

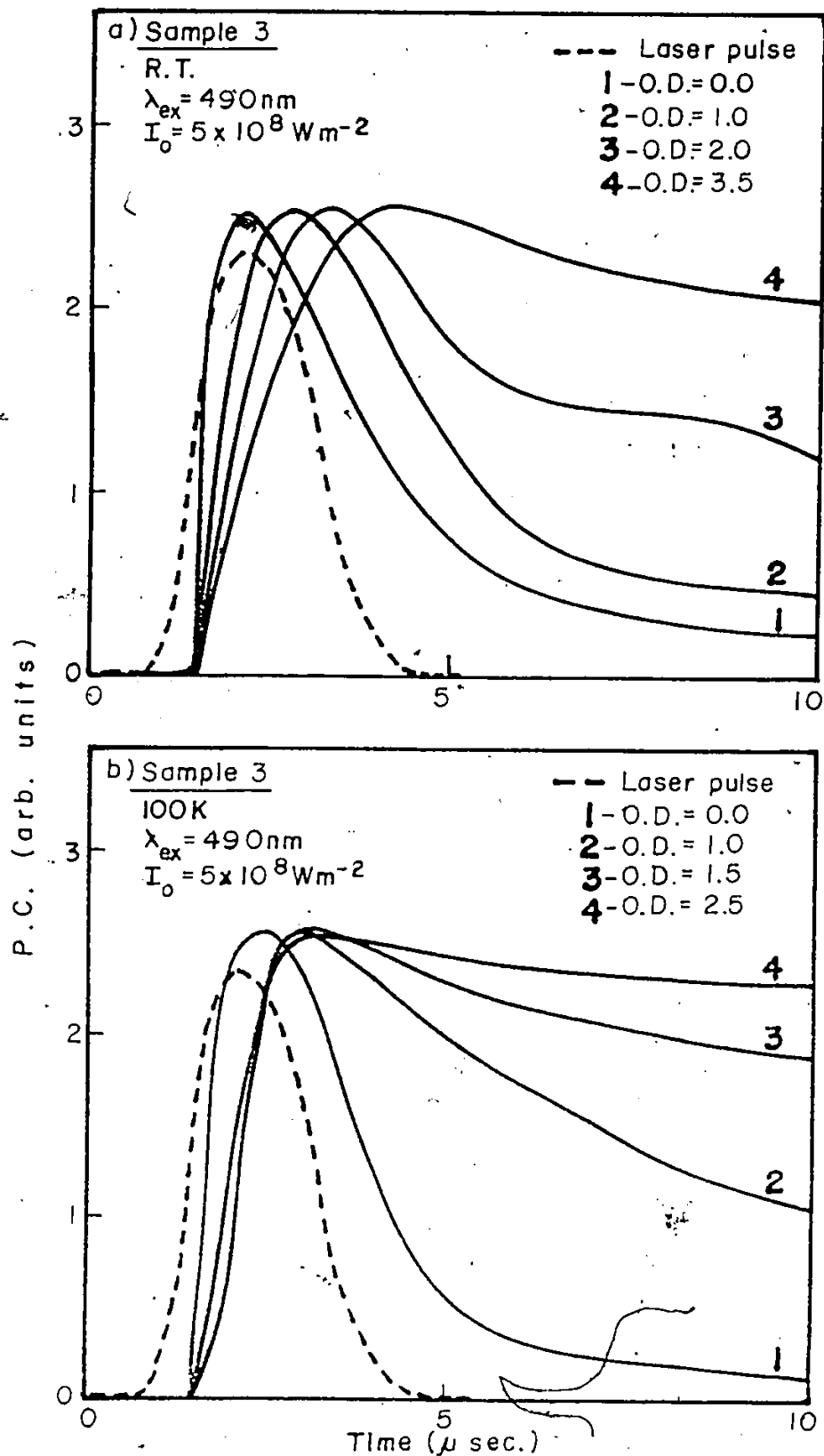


Figure 4.7 PC transient versus intensity at $\lambda = 490 \text{ nm}$ (high light) for Sample 3 a) RT and b) 100 K. (normalized)

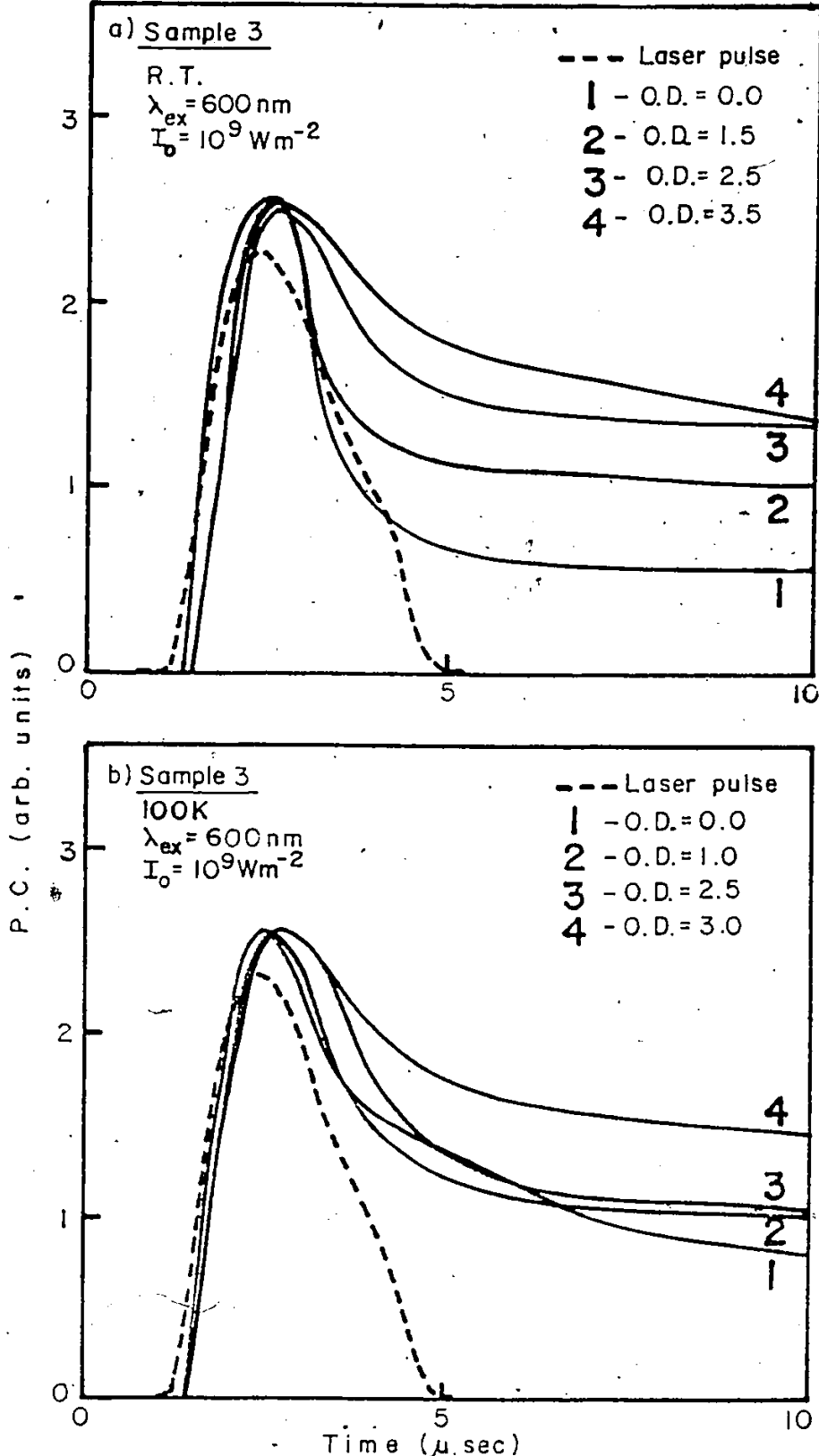


Figure 4.8 PC transient versus intensity at $\lambda = 600 \text{ nm}$ (high light) for Sample 3
 a) RT and b) 100 K. (normalized)

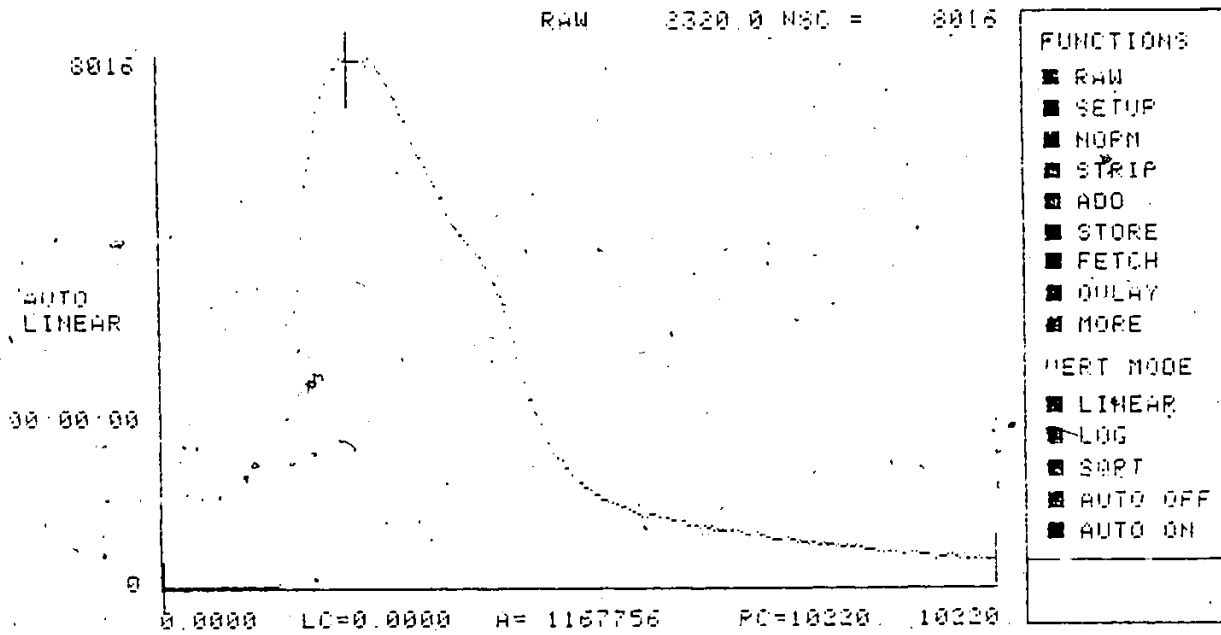


Figure 4.8c PC transient at 100K and $\lambda_{ex} = 490$ nm (raw data)

Table 4.3 Decay time of the PC transient at RT and 100 K for $\lambda = 490$ nm.

Sample 3:

Intensity (O.D.) ^a	$\lambda = 490$ nm	
	τ_D^* (μsec) ^b ($\pm 10\%$)	
	300 K	100 K
0	1.16	2.10
0.2	1.21	3.02
0.4	1.19	5.72
0.7	1.38	5.14
1.0	1.26	6.78
1.5	2.03	--- ^c
2.0	2.25	--- ^c

a. $I_0 = 5 \times 10^8$ w/m²

b. τ_D is taken from the maximum of the pulse to 60% of its maximum value.

c. no measurements taken at this O.D.

Laser Pulse decay time.

$\lambda = 490$ nm ; $\tau_D = 1.22$ μsec . $\pm 10\%$

Table 4.4 Rise time of the photocurrent response at RT and 100 K for
 $\lambda = 490$ and 600 nm.

Sample 3:

Intensity ^a (O.D.)	Rise Time (μ s) ^b ($\pm 10\%$)			
	$\lambda = 490$ nm		$\lambda = 600$ nm	
	300 K	100 K	300 K	100 K
0	0.66	0.86	1.06	1.06
0.2	0.82	0.88	1.06	1.10
0.4	0.96	1.14	1.08	1.06
0.7	1.18	1.20	1.05	1.12
1.0	1.34	1.60	1.08	1.16
1.5	1.52	1.72	1.06	1.22
2.0	1.86	1.98	1.10	1.32
2.5	2.42	1.96	1.26	1.32
3.0	2.50	2.20	1.34	1.48
3.5	2.82	2.24	1.22	1.48

a. $I_0 = 5 \times 10^8$ W/m² for $\lambda = 490$ nm and 1×10^9 W/m² for $\lambda = 600$ nm.

b. Laser pulse: $\lambda = 490$ nm $\tau_R = 1.20$ μ sec $\pm 10\%$
 $\lambda = 600$ nm $\tau_R = 1.00$ μ sec $\pm 10\%$

From the results obtained, the following three observations can be made:

- 1) The decay time, τ_D , of photoexcited carriers decreases with light intensity for the intrinsic excitation at both temperatures, whereas it is less strongly dependent upon intensity for the extrinsic case;
- 2) The decay time increases with decreasing temperature, and finally;
- 3) The rise time, τ_R , of the PC transient; i.e., the time it required to reach the maximum of photogenerated carriers, decreases with intensity for intrinsic excitation but remains almost constant for the extrinsic excitation.

Table 4.3 and 4.4 summarize the results obtained from the PC transient kinetics experiments. They show the decay and rise time of the PC signal at different intensities of excitation. The fact that the rise time and decay time of the PC transient be faster (in some cases) than the laser pulse itself may be explained by the uncertainty of the recorded laser pulse transient as explained in section 3.4.

The first two observations made are of crucial importance in the understanding of recombination processes. First, let us try to explain why the decay time decreases when the light intensity increases.

The following analysis will apply for band-to-band excitation. The same explanation can also be used for the extrinsic excitation and will be discussed later. As the light intensity increases more and more free electron-hole pairs are created. These free holes are then captured by the ionized acceptor levels E. At very high light intensity, most of these acceptor levels will be occupied by holes. On the other hand, the free electrons created have a large probability of being captured by the trapping levels T and subsequently recombine.

As is well known, the total-recombination process is the sum of the radiative and nonradiative recombination. In the case of CdIn_2S_4 at 100 K and 300 K, the radiative recombination is from transition 3 ($T \rightarrow E$) in figure 2.2 and the nonradiative one is proposed to be (section 4.6) band-to-band recombination and has a very fast decay time. Electrons can thus recombine via two pathways depending on their energy level; band-to-band or $T \rightarrow E$ recombination.

As previously discussed (section 2.2) as the intensity of excitation increases, the electron Fermi level also increases, which has the effect of filling the traps with electrons. Thus, the probability of traps emptying via the conduction band will be higher. Now, as the intensity decreases, the Fermi level also decreases, lowering the probability of thermal emptying of traps. Since the nonradiative recombination process is fast, the decay time of photoexcited carriers will be determined by the emptying of the traps. As previously discussed this emptying process can proceed via the $T \rightarrow E$ transition, where a photon is emitted, or by the absorption of thermal energy where the electrons are transferred into the conduction band. It is this emptying of the traps which is at the origin of the long tail (decay time) of the PC transient. Thus, the movement of the Fermi level with intensity is at the origin of the change in the PC decay time as a function of light intensity.

This effect was also seen at low temperature. The important difference between the PC transients at the two temperatures is that the decay time is much longer at 100 K than 300 K. This is again indicative of

the effect of trapping. Recall from section 2.1 that the major effect of trapping is to make the experimentally observed decay time of the photocurrent, after excitation has ceased, longer than the carrier lifetime. As the temperature is lowered, less thermal energy is available which decreases the probability of "de-trapping". Thus, the observed decay time is expected to become longer.

In the case of extrinsic excitation, the PC decay time is again a function of intensity and temperature but on a smaller scale as compared to the intrinsic excitation. The explanation used for intrinsic excitation could account for this behaviour, omitting the fact that holes are not created in the valence band but are directly generated in the acceptor level E. So, the hole capture process by the E-level is non-existent. This effect may be at the origin of the differences in the decay time between intrinsic and extrinsic excitation. Furthermore, one important point to emphasize is that the kinetics of the growth of the PC transient peak (at 600 nm) (τ_R) is independent of intensity, which is not the case for the intrinsic excitation. In the latter case, τ_R becomes longer as the intensity is decreased. At these low intensities, photocarriers are still being created even after the maximum of the pulse. As the intensity is increased, the PC rise time follows the pulse rise time. This effect was not as important in the extrinsic excitation. Because of this fast rise time, coupled with the fact that the maximum of the PC transient peak

is constant in time, it is assumed that a near steady-state condition is attained in the case of extrinsic excitation.

B. Intensity dependence of PC

It is known that the magnitude of the photoconductivity is governed by the rates of generation and recombination of nonequilibrium carriers. Two optical regions were used for high intensity PC excitation:

- 1) $\lambda = 490$ nm (Coumarin 102); to excite electrons across the gap; i.e., peak A.
- 2) $580 < \lambda < 620$ nm (Rhodamine 6G): to excite electrons from E-level to the conduction band (peak B).

The purpose of using the extrinsic excitation was to detect a PC saturation at high excitation light intensity which could be caused by an emptying of E-level. The band-to-band excitation was done to confirm these results.

As discussed previously (section 4.2), samples 1 and 3 can be considered to be of the same type, since their resistivities are comparable (a parameter related to the sulfur concentration). Sample 2 has a much higher resistivity and will be treated later.

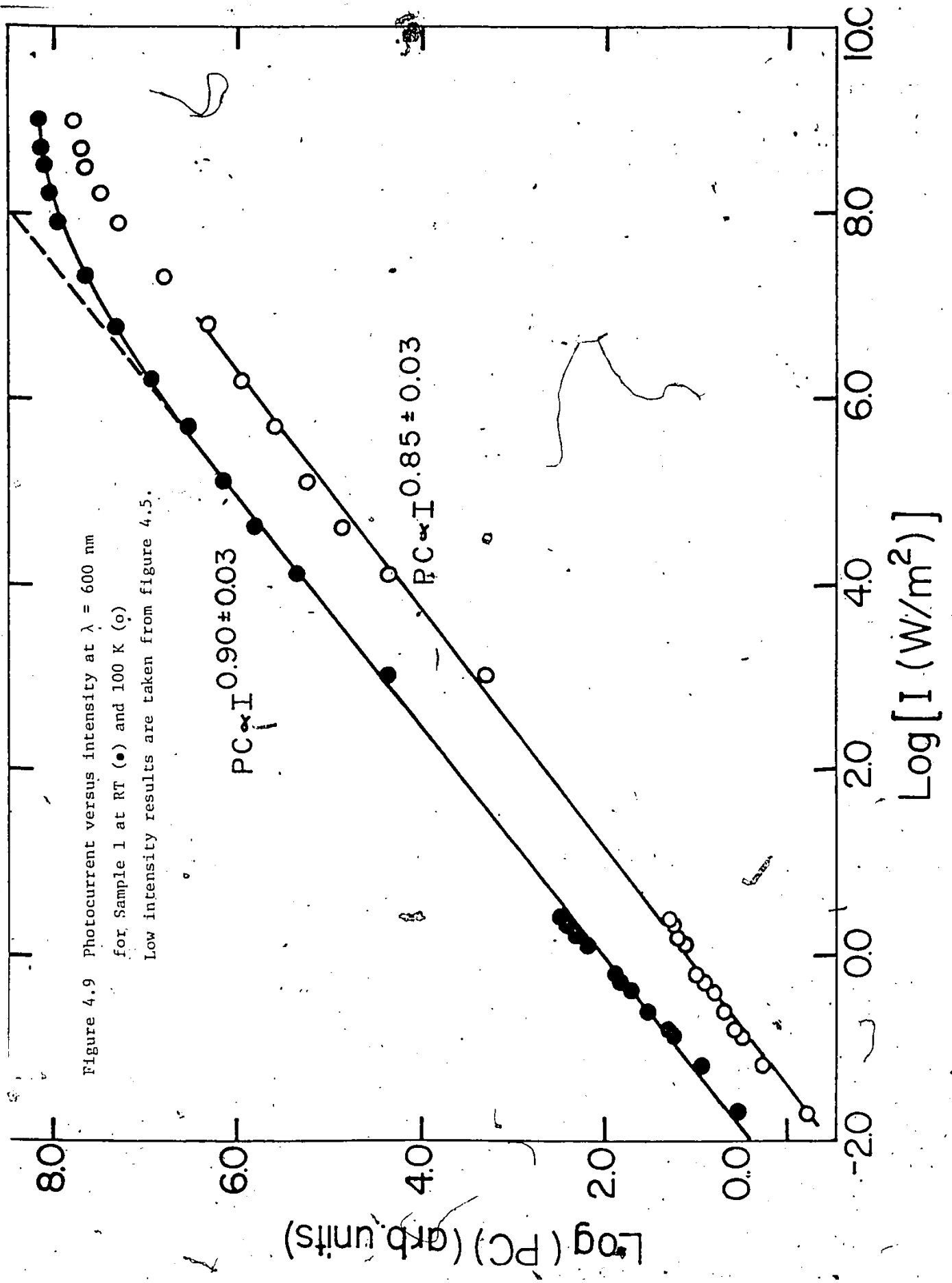
PC versus intensity measurements were performed for both Samples 1 and 3 in the region of peak B (transition 2) in an attempt to observe saturation effects. In that low absorption region ($\alpha d \ll 1$), carriers are generated over the entire thickness, d , of the sample and the generation rate is proportional to the absorption coefficient (see Theory section 2.1).

Figure 4.9 shows the photocurrent as a function of light intensity for Sample 1 at RT and 100 K at an excitation wavelength of 600 nm for intensities up to 10^9 W/m². The damage threshold was determined to be 10^{11} W/m². The highest intensities (10^{11} W/m²) were obtained by focussing the beam on the sample. At both temperatures, a sublinear dependence of the PC response at low values of light intensity was observed (figure 4.5 (a)); however, as the light intensity increased, a marked deviation from sublinearity was apparent, eventually attaining a plateau. This saturation effect is more easily seen in Figure 4.10 - an enlargement of Figure 4.9 showing the PC values at the highest light intensities.

The saturation effect, believed to be caused by an emptying of the acceptor levels, E, at high light intensities, is seen at both temperatures: however, it is more prominent at 300 K. Two phenomena might explain the difference between 300 K and 100 K:

1) The relaxation rate, which governs the regeneration of the acceptor levels, is not necessarily the same at both temperatures. In other words, the luminescent transition $T \rightarrow E$ is more efficient at 100 K than at 300 K (as will be discussed in section 4.6). Since this radiative recombination is fast (vide infra) more electrons will be restored in the E-level at low temperature by the time the PC transient reach its maximum.

2) The absorption coefficient at $\lambda = 600$ nm decreases from $\alpha = 3$ cm⁻¹ at RT to $\alpha = 1$ cm⁻¹ at 100 K⁽³⁰⁾ (see appendix B). This decrease in α would have the effect of masking the saturation, since less photons would be absorbed at 100 K than 300 K for the same intensity.



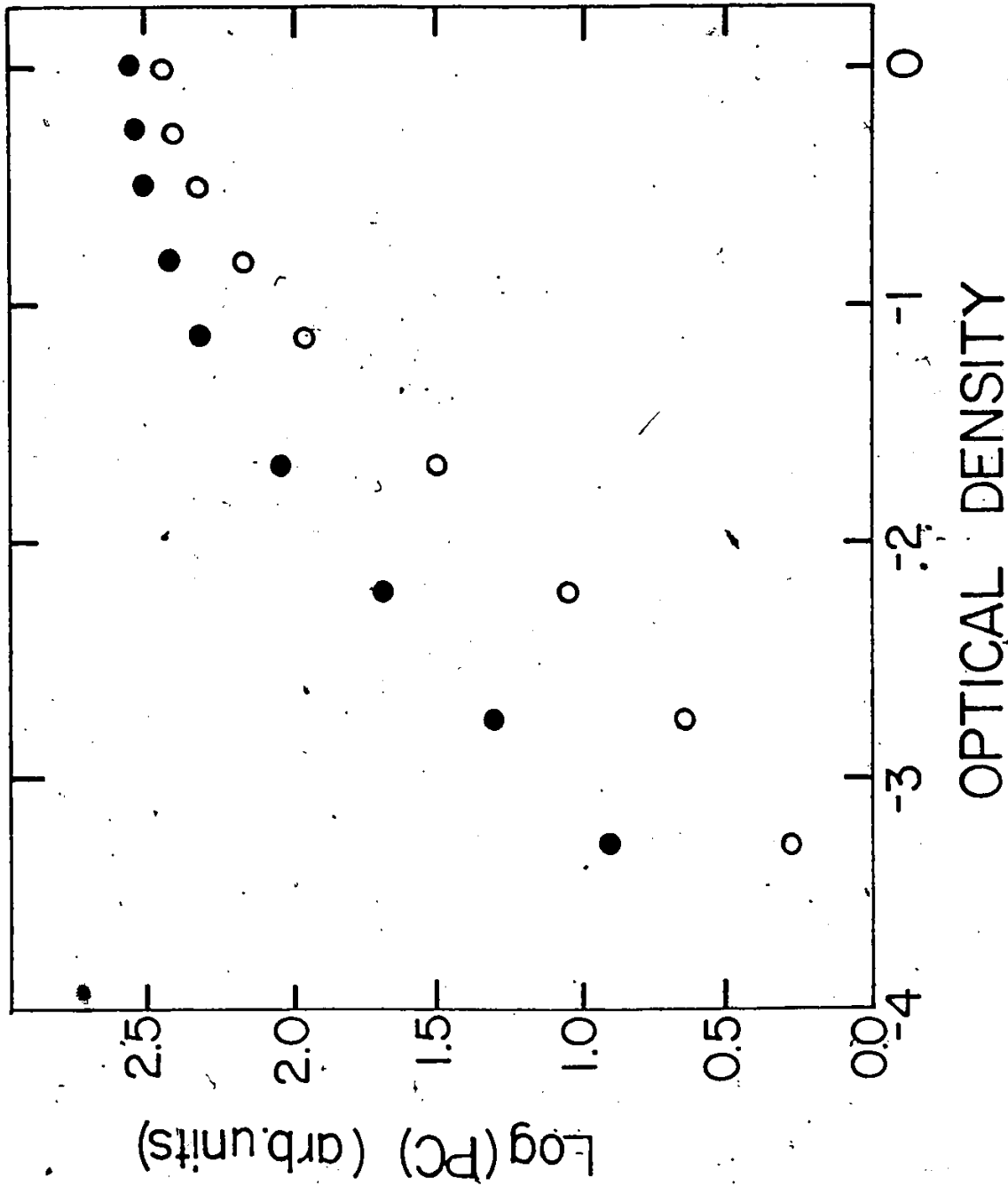


Figure 4.10 Photocurrent versus intensity at $\lambda = 600$ nm for Sample 1 at RT (\bullet) and 100 K (\circ)

A saturation of impurity PC at high intensity has also been reported for GaSe by Abdullaev and coworkers⁽³⁶⁾ and by Celler and coworkers⁽³⁷⁾ in n-GaAs. Their results were quite different from ours. Since they were exciting electrons from a level which was also the primary recombination center, increasing the intensity had the two fold effect of saturating the generation rate and increasing the recombination rate. In the case of CdIn₂S₄ samples, the saturation effect observed over a broad spectral range (585 - 615 nm), corresponding to peak B, is caused solely by an emptying of E-levels. The lifetime of the excited carriers can be considered constant for the 600 nm excitation as demonstrated by the PC transient results (fig. 4.8). The fact that the rise time of the PC response follows the pulse rise time, indicates that the lifetime of the photogenerated carriers is less than or equal to the laser pulse. Thus, equilibrium at the maximum of the PC transient is obtained.

The above data were obtained on Sample 1. In comparison, the saturation effects were less apparent for Sample 3 (see Figure 4.11). This difference can best be explained by inspection of the low-intensity PC spectra of Figure 4.2 and 4.4. In Sample 3, the fact that peak B is relatively more intense at both RT and 100 K indicates a greater density of acceptor levels E, making saturation more difficult to achieve. From Figure 4.9, it is possible to estimate the density of acceptor levels E, assuming the free lifetime of the photocarriers to be constant and of the order of the laser pulse width. It is necessary to calculate only the number of photons absorbed per unit volume at the saturation point. The

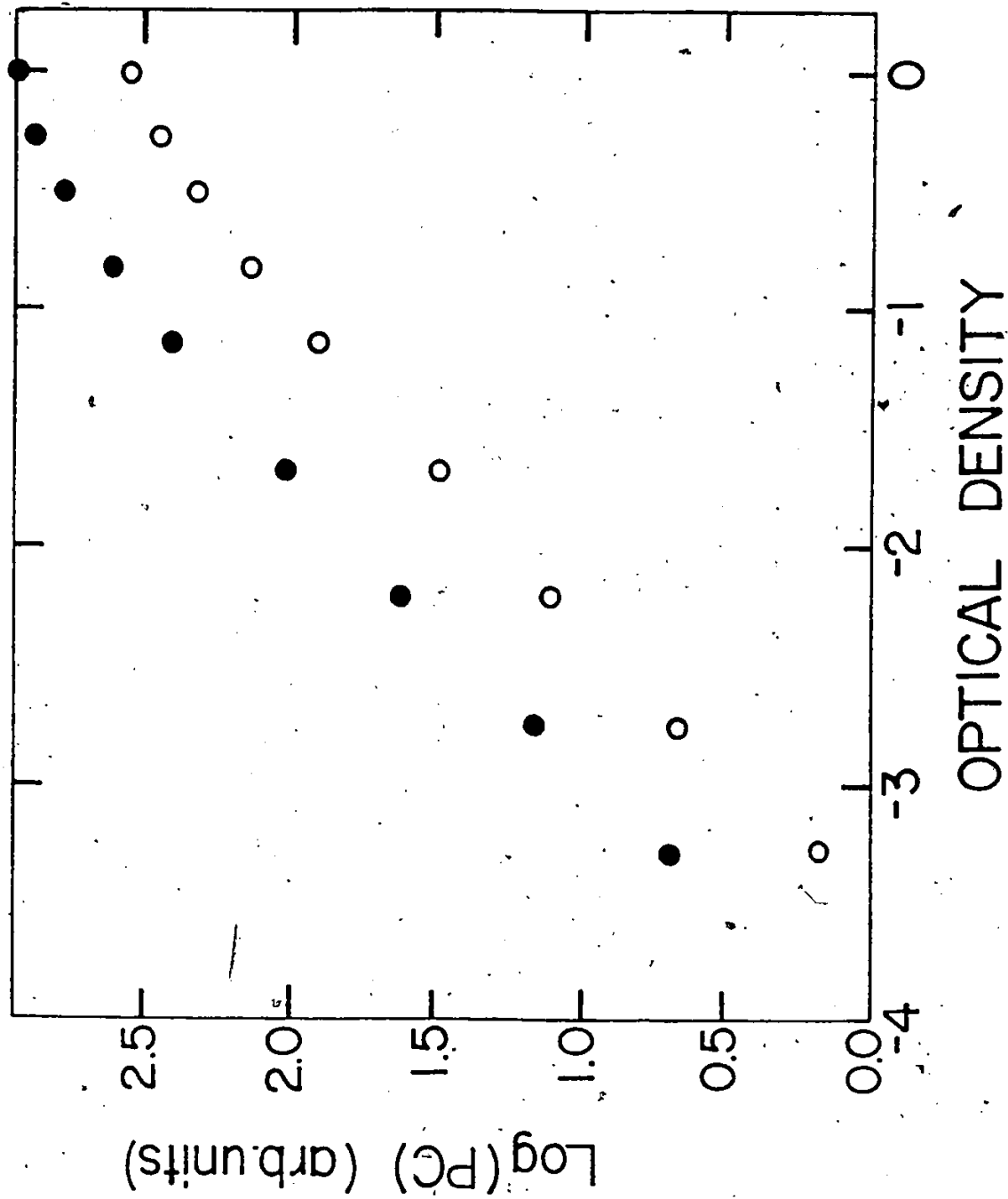


Figure 4.11 Photocurrent versus intensity at $\lambda = 600$ nm for Sample 3 at RT (●) and 100 K (○)

saturation at RT occurs at an intensity of $I_0 = 1 \times 10^9 \text{ W/m}^2$ at 600 nm. The number of acceptors can be calculated to first order as follows:

$$\begin{aligned} N_A &= I_0 (1-T-R) \Delta t/h\nu d \\ &= \alpha I_0 \Delta t/h\nu \end{aligned}$$

where $\alpha = 3 \text{ cm}^{-1}$ and $R_0 = 0.2$ at $\lambda = 600 \text{ nm}$, Δt being the laser pulse width, $h\nu$ is the energy of a photon in joules and T, R the transmission and reflection coefficient respectively. This equation was derived in section 2.1.

The calculated density of acceptors was found to be $N_A = 2 \times 10^{18} \text{ cm}^{-3}$. Since the acceptor E₁ and trap T originate from Cd-In lattice exchange, the calculated density of the acceptors should be of the same order as (or, if complete compensation is not achieved, less than) that of the traps. The latter value was also determined by Endo et al.⁽³⁸⁾ and Anedda et al.⁽⁸⁾ and their values are in quantitative agreement with the value of N_A obtained here. In the present analysis we have assumed that there is no contribution to photocurrent from a change in the electron mobility due to the change in the charge status of the defects. This is a fair approximation at RT where scattering from charged impurities is not very important.

In comparison with samples 1 and 3, sample 2 has a lower sulfur concentration and therefore a higher resistivity. For the PC versus the intensity experiments at RT and 100 K for the extrinsic excitation of 600 nm, a linear dependence was observed. However, no saturation was detected at either temperature. The reason for this is the same as before. The concentration of E-level in sample 2 is greater than in sample 1. This

is taken from the ratio of peak B to peak A (figure 4.2 and 4.3) which gave a lower value in the first sample. Another reason for this could be due to the high concentration of V-centers. Because of this, the Fermi level would lie higher in the gap, and the tunneling process $T \rightarrow V$, explained in section 4.1 would be more probable, which would have the effect of filling some of the traps. As electrons would be pumped from the E level to the CB, some of the electrons already trapped could decay into the E-centers via transition 3, and thus no emptying could be observed.

Finally, PC versus intensity experiments were performed at 490 nm. In this case, a sublinear dependence was observed over the entire excitation intensity for the three samples. No saturation effect was observed at high excitation light intensity. If it is assumed that the excitation light intensity at 490 and 600 nm affects the carrier decay time in the same way, as was demonstrated by the PC transient results, then this is a good indication that the PC saturation observed at 600 nm was due to an emptying of E-level and was not related to a lifetime effect. The inability to saturate with intrinsic excitation is reasonable since the valence band must be emptied first and this is not achieved as readily.

An irrefutable experiment to prove that the saturation of PC in the extrinsic region resulted from the emptying of E level would be the saturation of the absorption coefficient at high light intensity, and this is the subject of the next section.

4.5 Intensity - dependent absorption

Measurements of intensity-dependent absorption were attempted to supplement interpretation of PC saturation. As explained in section 3.3, a dye laser was used as the excitation source. The exciting radiation was in the form of single pulses of 2 μ sec duration in the spectral range 590 - 620 nm. A set of calibrated neutral density filters was used to vary the excitation intensity. The transmitted intensity was measured by a photomultiplier coupled to a multichannel averager. It is important to note that data were obtained by measurement of the intensity-dependent transmission, so that only a small change in a large quantity, the transmissivity, is detected. The variation of the signal detected by the PM would in fact be due to the variation of the coefficient of absorption of the crystal. The intensity-dependent transmission was investigated in the optical region of peak B. The first thing measured was the absorption coefficient at these wavelengths, at low intensity.

For this, two samples of different thickness were used and for small incident intensities, the transmitted intensity varies linearly with I_0 as expected with the dependence

$$I = \frac{(1 - R_0)^2 e^{-\alpha d} I_0}{1 - R_0^2 e^{-2\alpha d}}$$

where R_0 is the reflectivity ($R_0 = 0.2$ at $\lambda = 600 \text{ nm}^{(31)}$), α the absorption coefficient, and d the sample thickness. The transmitted intensity was

measured by a silicon detector. The signal measured was directly proportional to the transmitted intensity. By using two different sample thicknesses, we have:

$$\frac{I_1}{I_2} = \frac{(0.8)^2 e^{-\alpha d_1} [1 - (0.2)^2 e^{-2\alpha d_2}]}{(0.8)^2 e^{-\alpha d_2} [1 - (0.2)^2 e^{-2\alpha d_1}]}$$

$$= e^{-\alpha(d_1 - d_2)} \left[\frac{1 - 0.04e^{-2\alpha d_2}}{1 - 0.04e^{-2\alpha d_1}} \right]$$

but in this optical region, $\alpha d \ll 1$ so that the term in brackets is essentially equal to one.

Finally,

$$\frac{I_1}{I_2} = e^{-\alpha(d_1 - d_2)}$$

where, in our case, $d_1 = 0.066$ cm; $d_2 = 0.076$ cm; $I_1 = 11.35$ mV; and, $I_2 = 11.0$ mV, so that

$$\alpha = \frac{1}{(d_2 - d_1)} \ln \frac{I_1}{I_2}$$

which gives $\alpha = 3.2 \text{ cm}^{-1}$ at 600 nm in good agreement with Nakanishi et al. (29). A low absorption coefficient was expected since this wavelength corresponds to an extrinsic transition.

At high intensity, the transmission of the sample is expected to increase with increasing intensity because of the tendency of the absorption to saturate. The transition responsible for a saturation in CdIn_2S_4 could be represented as follows: (see Figure 2.2). A reduction in the linear absorption represented by the transition 2 (from an ionized acceptor to the conduction band) could have occurred because of emptying of the acceptor levels. An increase in the excitation intensity would result in gradual saturation of the absorption at that wavelength since no more electrons would be available to absorb the photons, so that the material would become transparent to the incoming light. This saturation effect is the same phenomena as that which is explained in the previous section.

In principle, optical absorption versus intensity measurements in the extrinsic range should have complimented the PC saturation measurements but comparisons are difficult because of the low contrast involved in the $\alpha d \ll 1$ range. The reason why the saturation was easily observed by photoconductivity in contrast to absorption is simply because two different quantities were measured. In the case of PC, the number of photons absorbed by electrons were investigated but for the absorption experiment, we were actually looking at the photons not being absorbed by the material, i.e., the transmissivity. For example, with a sample thickness on the order of 0.076 cm and an absorption coefficient of 3 cm^{-1} at low light intensity decreasing to say 1.5 cm^{-1} at high intensity (as is predicted by theory), the real change in transmission recorded would be of the order of

$$1 - \frac{I_1}{I_2} = 1 - \frac{I_0 e^{-\alpha_1 d}}{I_0 e^{-\alpha_2 d}} = 1 - e^{-0.076(1.5)} = 10\%$$

which is a small quantity to measure. This is the reason why the photoconductivity seems to be a more powerful technique for the detection of saturation effects in the extrinsic region, since PC is directly proportional to the absorption coefficient.

There were some experimental problems to be overcome before attempting the transmission experiments. The path of the laser beam was changed when filters were added to or removed from the front of the sample since the filters were not all perfectly parallel to each other. This path change was enough to cause a deflection of the beam from the center of the 800 μm hole (where the sample sat) to the edge, producing unprecise results. To solve this problem, the optical cryostat was mounted on an X-Y-Z translation system. By maximizing the signal each time a filter was moved (i.e., by moving the cryostat), it was possible to obtain more or less reproducible results, the uncertainty being of the order of $\pm 10\%$. As a result, nothing could be concluded from the absorption coefficients measured by this technique.

4.6 Photoluminescence versus intensity and PL transient kinetics

As demonstrated in a previous section, a saturation of PC signal with intensity was observed. The cause of this saturation was attributed to an emptying of the acceptor level E. This saturation effect could

produce interesting features because of population inversion between levels E and T.

PL versus intensity experiments were done in the hope of detecting stimulated emission in CdIn_2S_4 material. This stimulated emission would be characterized by a drastic increase of the measured light output (luminescence) at the point where stimulated emission becomes important. But first let us start with some luminescence time decay measurements. The PL transients provide useful information on the kinetics of recombination as well as the capture cross sections of some levels.

Where radiative decay is the only possible decay mechanism, a measurement of the luminescence decay time can provide a measure of the radiative lifetime of excited state of the crystal. More typically, the measurement of luminescence decay time, τ_L , does not provide a direct measurement of radiative lifetime because of rapid decay via other mechanisms. For the case where nonradiative decay is faster, the measured decay rate is characteristic of the nonradiative processes. This situation is typical for recombination from intrinsic states of semiconductors (band-to-band recombination) and particularly in the case of indirect gap materials, where the nonradiative recombination rate can be orders of magnitude faster than the radiative rate.

Luminescence decay time, τ_L , in the simplest case, involves a 2-level system, where the ground state is designated by Z and the excited state by Z^* . Let us assume that the transition $Z^* \rightarrow Z$ is radiative. When the exciting photons have sufficient energy, electrons are excited from the

Z to the Z^* level. Afterwards, the electrons will relax back to their ground state, emitting photons with energy equal to the difference in energy between the Z^* and Z level. This luminescence process is known as fluorescence. In this case, τ_L is simply the time taken by the electrons to relax from the Z^* to the Z level.

Now let us introduce a third level, X, which acts as a trap for excited electrons and sits near the excited state Z^* . The following assumptions may be made about these levels: 1) the "trapping" transition $Z^* \rightarrow X$ is considered nonradiative; 2) the emission of the trapped electrons to the excited state Z^* must be phonon assisted; 3) the transition $X \rightarrow Z$ is a radiative one; and, 4) the transition $Z^* \rightarrow Z$ is still a radiative one. Again, after excitation ($Z \rightarrow Z^*$), some of the electrons will decay back radiatively to the ground state ($Z^* \rightarrow Z$; fluorescence) and some of them will be trapped ($Z^* \rightarrow X$). From the traps level X, the electrons can either make the radiative transition $X \rightarrow Z$ or be re-emitted in the excited level Z^* ($X \rightarrow Z^*$) by the absorption of thermal energy. The first transition ($X \rightarrow Z$) is commonly known as phosphorescence. As for the remaining electrons in the Z^* level, they can make the final radiative transition $Z^* \rightarrow Z$, returning to their ground state. This process is known as delayed fluorescence. In the present model, τ_L is expected to be longer than the one found in the 2-level system because of the time spent by the electrons in the traps. Obviously, the deeper the traps are (or the lower is the temperature), the longer the decay time will be. In summary, the lumi-

nescence decay time is simply the time taken by all the electrons to go back to their ground state, after excitation, by any way available to them.

As will be seen presently, CdIn_2S_4 exhibits phosphorescence rather than fluorescence. Figure 4.12 shows the photoluminescence transient of sample 3 at (a) RT and (b) 100 K for band-to-band excitation. The spectrometer was set to observe the maximum of the L luminescent band (Transition T \rightarrow E). It is important to notice that the luminescence decay time, τ_L , decreases slightly with increasing light intensity at both temperatures (see figure 4.12). Moreover, a net increase in the decay time is apparent when the temperature is dropped from 300 to 100 K. Finally, the luminescence efficiency, η , was observed to be inversely proportional to temperature. The explanation of these three phenomena requires the presence of a nonradiative recombination process as suggested by Grilli et al⁽¹³⁾. There exists a competition between the radiative transitions (T \rightarrow E), where the probability P_r depends very slightly on temperature, and the nonradiative transitions, where the probability P_{nr} increases with temperature. We propose this nonradiative transition to be from the conduction band to the valence band. The lifetime of the luminescence is proportional to $1/P_r$, but the measured luminescence decay time, τ_L , is given by⁽³⁹⁾:

$$\frac{1}{\tau_L} = P_r + P_{nr}$$

At low temperature, P_{nr} is almost zero; hence, the luminescence decay time is simply given by the inverse of the radiative transition probability, P_r .

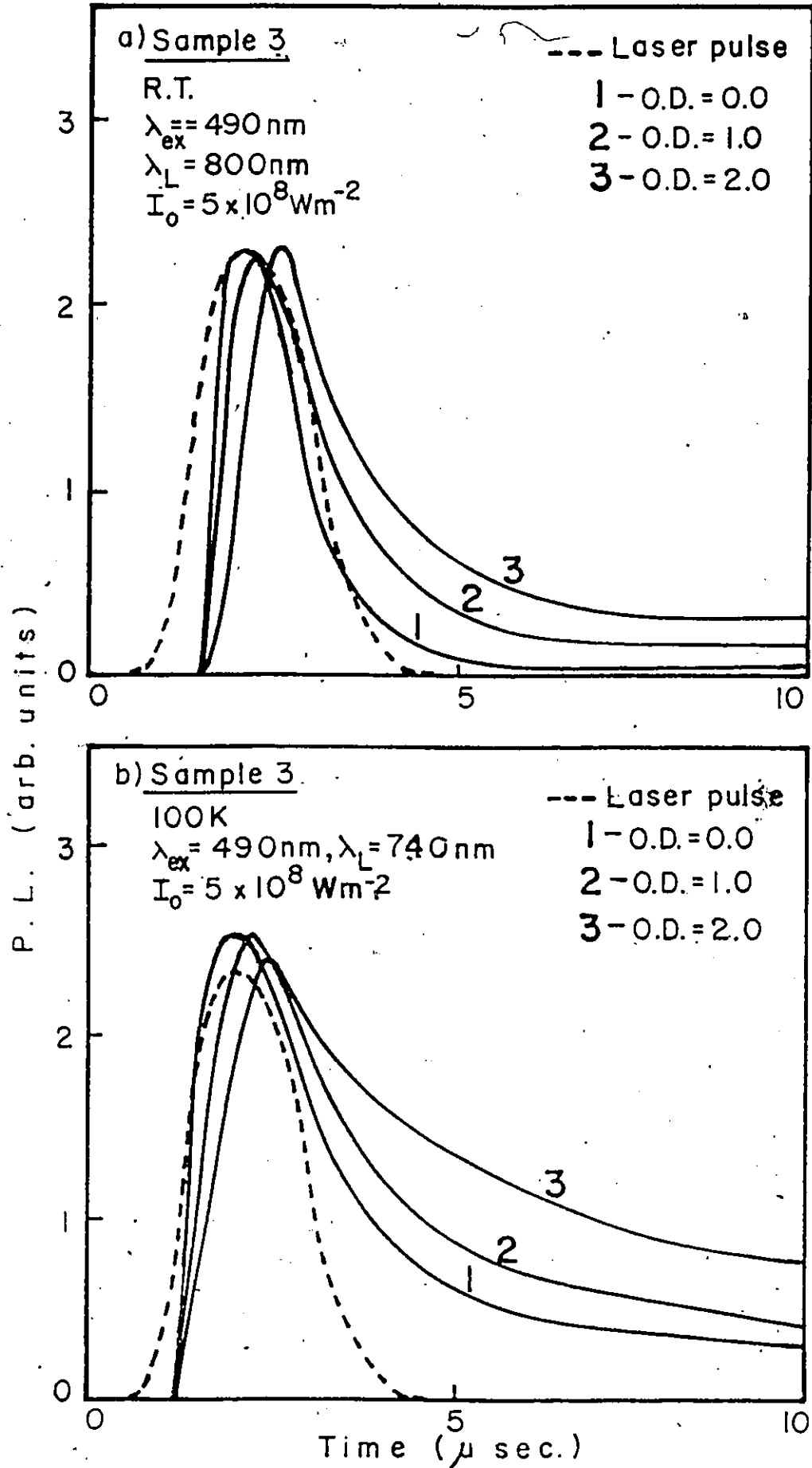


Figure 4.12 PL transient versus intensity at $\lambda = 490 \text{ nm}$ (high light)

As the temperature is increased, the nonradiative recombination rate starts to become more significant and thus τ_L is expected to decrease. In terms of CdIn_2S_4 band diagram (figure 2.2), electrons are excited from the valence band (VB) to the conduction band (CB) where they can either remain there (CB) or be trapped by the T-centers. At low temperatures, the nonradiative CB \rightarrow VB transition is very unlikely to occur, thus relaxation of the excited electrons must be via transition 3 (T \rightarrow E), giving radiative recombination (L luminescence band). Furthermore, even if there exists a competition between radiative and nonradiative transitions at 100 K, because the thermal energy is very small, the probability of trap emptying (T \rightarrow CB) is very small, much smaller than at RT. Hence the electrons will remain in the traps for a longer period and decay via transition 3. Thus, the luminescence efficiency, η , will be higher at low temperature, because nonradiative transitions are unlikely to occur. On the other hand, at higher temperatures (RT) the nonradiative recombination rate (CB \rightarrow VB) contributes significantly to the total recombination process so that excited electrons in the CB can either recombine with a free hole in the VB or be trapped by the T-level. From this level, the electrons can again decay via transition 3 or be re-emitted in the CB (because of higher thermal energy) and again recombine nonradiatively. This is basically the same three level system which was discussed for phosphorescence. The change in the luminescence decay time, τ_L , and luminescence efficiency, η , with temperature can thus be explained from the above model.

A slight decrease in the decay time was also observed as the

exciting light intensity was increased. This behaviour could simply be due to a local heating by the laser beam at higher intensities which would have the same effect as previously mentioned. Another, more likely, explanation could be that there is a rise of the Fermi level with intensity. As the intensity is increased, the Fermi level sits higher in the traps, making the probability of the trap emptying higher, and thus a shorter decay time could be observed.

An important point to notice from figure 4.12 is that the rise and decay times of some PL transient curves are faster than the laser pulse. This unusual process is also seen in flash-lamp pump dye laser where the laser pulse is faster than the pump (flash-lamp) itself. This observation is a good evidence for stimulated emission in our crystals.

There exist many similarities between the PC and PL transients. In both cases the decay time decreases with increasing temperature and with increasing intensity of excitation. The comparison of figure 4.12 with 4.7 shows that the PL transient is much faster than the PC. This point exemplifies what was said in the theory (section 2.3) concerning the two processes: in materials which show both luminescence emission and PC, the rate of decay of the luminescence emission is appreciably more rapid than the decay of the PC. In other words, good luminescent materials require rapid recombination, whereas good photoconductors require slow recombination. To repeat what was said earlier in section 2.3, it is possible to distinguish two possibilities: a) Both luminescence and PC are associated with the capture of the same type of carriers, either electron or hole, and b) luminescence is associated with the capture of one type of carrier, but PC with the capture of the other type of carrier. In the former case (a), it seems that the presence of good luminescence emissions is indicative of favorable center for PC. This is because the capture cross section of

known excited luminescence centers may be rather small, much smaller than the cross section of "poison" centers for luminescence, i.e., centers which can dissipate the energy of the excited carrier nonradiatively. Thus the density of large cross section centers is small, and freed charge carriers will have a reasonably long lifetime before recombination. In the latter case (b), the requirements for good luminescent materials and those for good photoconductors are closely related. Centers are required which would have both a large cross section for minority carriers producing the emission, and then a small cross section for majority carrier, producing long free lifetime for the majority carriers. In a n-type material like CdIn_2S_4 , a mixture of case (a) and (b) are more likely to be true. In summary, a disparity in decay time between luminescence and PC, would result directly from situation (b), and could also be found under conditions described in situation (a) if some of the optically created minority carriers were captured at centers with a smaller cross section than the luminescence centers.

Let us summarize the above discussion in terms of the band structure of CdIn_2S_4 (figure 2.2). From the PC and PL transient results, it can be predicted that the capture cross section of the ionized acceptor level E for free holes is large since when the excitation energy is greater or equal to the band gap, the luminescent transition $T \rightarrow E$ is seen (L-band). This proves that the E-level must catch a free hole, located in the valence band, in a very efficient way. Moreover, when the wavelength of the

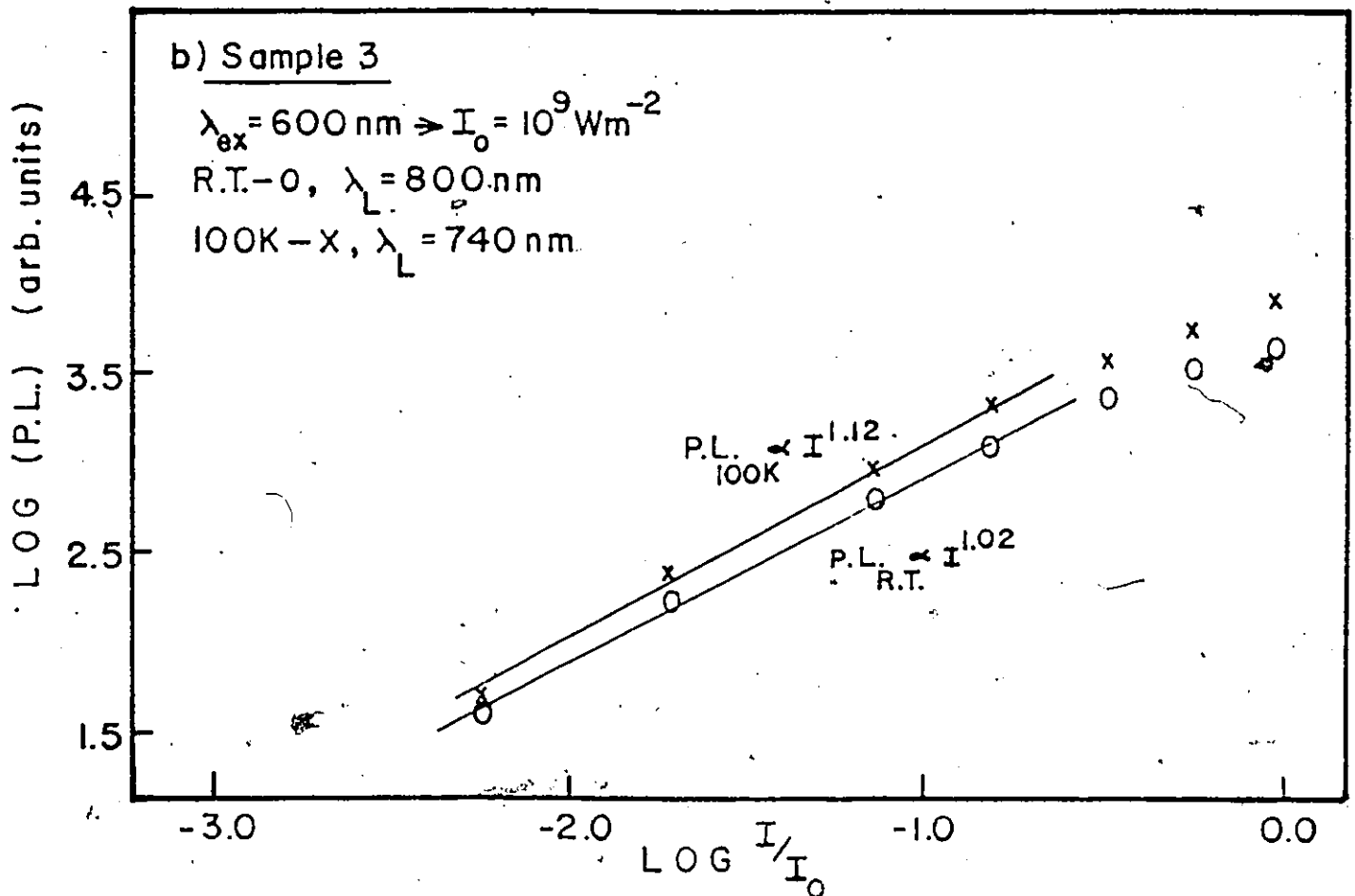
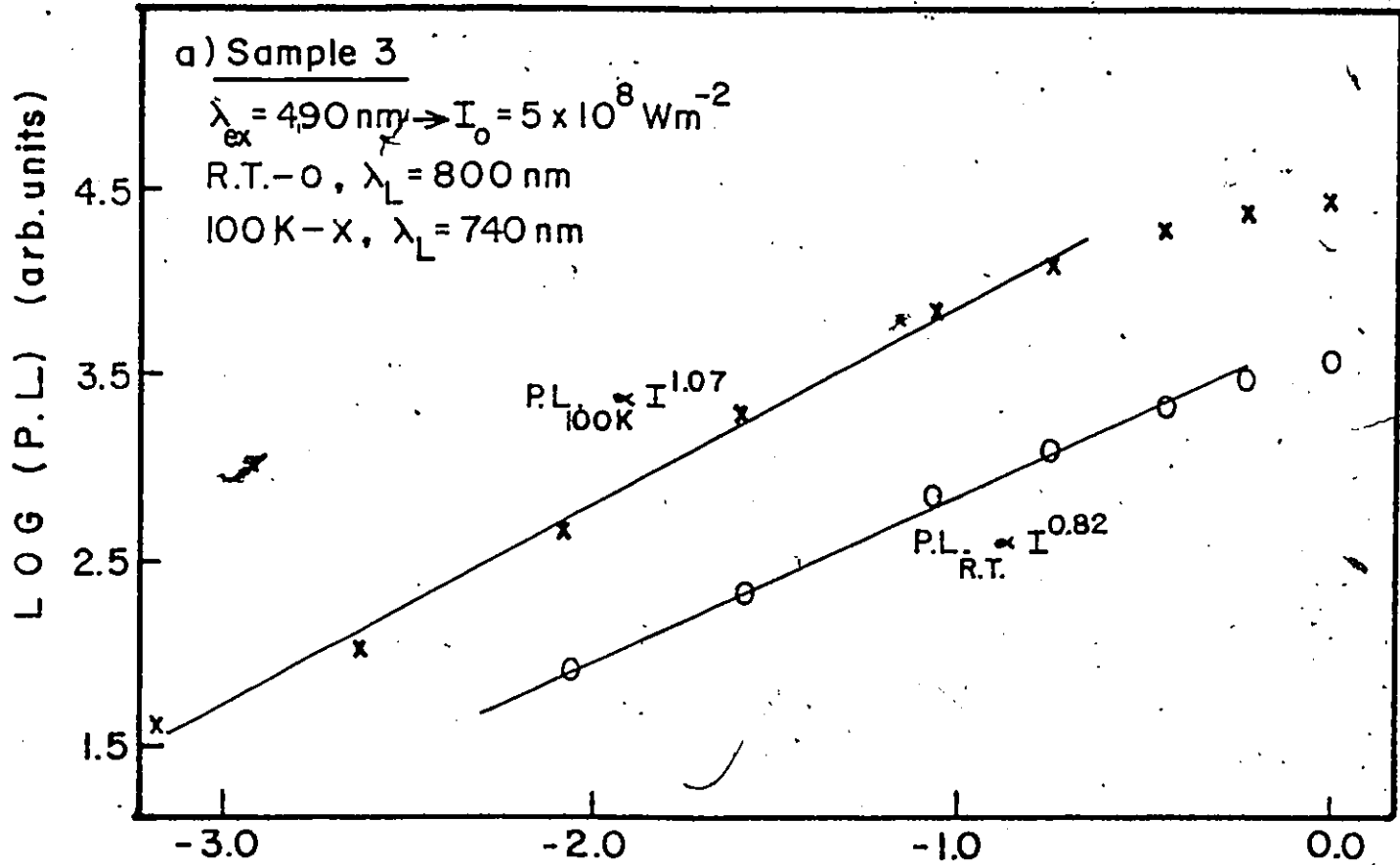
excitation light is 600 nm (transition 2 in figure 2.2), exactly the same $T \rightarrow E$ transition is seen in the luminescence spectra, as explained in section 4.1.

As far as the PL transient is concerned, band-to-band excitation and excitation at 600 nm have similar characteristics, and can be explained by the same process. Luminescence decay time decreases with temperature and intensity of excitation.

Finally, let us look at the PL response versus intensity of excitation. This experiment was carried out at both temperatures for transition 1 (band-to-band) and transition 2 (E-level to CB) (see figure 2.2). The results are shown in figure 4.13. The maximum of the L-luminescence emission band at each of the temperatures was chosen (800 nm at RT and 740 nm at 100 K). In three out of four cases, a superlinear behaviour was observed at low light intensities. At higher intensities a break in the superlinear behaviour is observed, producing then a sublinear dependence. The explanation of this dependence is as follows. The L-band luminescence in CdIn_2S_4 consists of donor-acceptor (D-A) transitions⁽¹³⁾ where the donors are the T-levels and acceptors the E-level. A D-A transition involves an electron bound to the donor and a hole bound to the acceptor. The radiative probability for such transitions depends on the overlap of the wavefunctions of the electron at the donor and the hole at the acceptor and is rather small. However, at low temperatures, the carriers cannot escape once they are captured at these impurities and D-A pair transitions become one of the dominant radiative processes. D-A

Figure 4.13 Photoluminescence versus intensity for Sample 3

a) $\lambda_{ex} = 490 \text{ nm}$ and b) $\lambda_{ex} = 600 \text{ nm}$
 error on slope: a) ± 0.03 , b) ± 0.07



transitions can explain both the sublinear ($\alpha < 1$) and superlinear ($1 < \alpha < 2$) behaviour observed. For example, the sublinear dependence at high light intensity may be explained by the fact that more of these D-A pairs are created, reaching a "saturation point" when no more ionized centers are available, causing a decrease in the slope.

It should be remembered that these are only preliminary results. Additional experiments are currently underway both to confirm these results and to provide a greater understanding of these processes.

V. SUMMARY AND CONCLUSION

The present research was undertaken in order to study the photoconductivity and photoluminescence of CdIn_2S_4 crystals under high excitation intensities. The PC and PL spectra, at low light intensities, were obtained at different temperatures and good agreement was found with the energy band diagram previously proposed for CdIn_2S_4 crystals⁽¹³⁾.

The intrinsic and extrinsic photoconductivity of CdIn_2S_4 was studied at 300 K and 100 K as a function of light intensity over twelve orders of magnitude and very interesting results were obtained. The linear and sublinear behaviour observed at both temperatures for low intensity intrinsic and extrinsic excitation could be explained by the existence of an exponential energy distribution of traps and follows the theoretical model proposed. Saturation of impurity PC observed in the extrinsic region under high intensity light allowed us to determine the density of the defects which are presumably responsible for the absorption in CdIn_2S_4 at 600 nm. The PC saturation implies that the supply of electrons in the level E is not appreciably restored by direct laser activation or by thermal activation from the valence band. The absence of such an effect was attributed to a relatively high cross section of the unionized E-level for free hole capture, as demonstrated by the PL-transient experiment.

That the PC saturation was due to an emptying of the E-level and was not caused by a change in lifetime with intensity was confirmed by the PC transient experiment. This experiment was performed at both temperatures for the 490 nm and 600 nm excitation wavelength. The decay time of photo-

excited carriers was deduced and analysed as a function of light intensity. The results were attributed to the presence of trapping levels near the conduction band and the movement of the Fermi level with temperature and intensity of excitation.

Finally, the photoluminescence experiments at high intensities were performed. First, the PL transient experiments were investigated at different intensities and temperatures. From these results, information about capture cross section of the E and T-levels was obtained. Furthermore, a model for the radiative and nonradiative recombination processes was proposed and applied to explain these results. The dependence of PL intensity on excitation light intensity was determined in the hopes of observing stimulated emission. Unfortunately, there was no evidence of stimulated emission probably because the available samples did not exhibit marked PC saturation (sample 1 was destroyed before PL experiments could be done).

CdIn_2S_4 could display interesting effects resulting from population inversion between levels E and T. This material could be used in a tunable solid state laser in the near infrared region of 1.4 to 1.8 eV because of the high density of traps and their spread in energy. All this would be possible providing that an inversion of population could be achieved. The three levels for this laser would be as follows:

- 1) Level E: ground state
- 2) Conduction band: excited state
- 3) Trap T: metastable state

The excitation source could be provided by a high intensity laser, pumping the electrons from the E level to the CB. The majority of the electrons would be trapped in level T and then decay back to level E emitting photons with energy 1.6 ± 0.2 eV. This process is of the same kind as that used in the organic dye laser. So, CdIn_2S_4 would be a solid state equivalent of a liquid dye such as Rhodamine 6G and its efficiency would be inversely proportional to temperature.

Further experiments could be done on some new CdIn_2S_4 crystals. The first thing would be to choose a sample which shows a small amount of extrinsic disorder; i.e., a low concentration of E-level. If the samples showed a saturation of PC for high intensity, the dependence of PL on light intensity could be explored to see if the predicted stimulated emission does occur.

APPENDIX A

$$\lim_{\alpha d \ll 1} [1 - T - R] \rightarrow \alpha d$$

Let $\alpha d = x$

$$1 - T - R = 1 - \frac{(1-R_0)^2 e^{-x}}{1-R_0^2 e^{-2x}} - R_0 \left\{ 1 + \frac{(1-R_0)^2 e^{-2x}}{1-R_0^2 e^{-2x}} \right\}$$

$$= (1-R_0) \left\{ 1 - \frac{(1-R_0) e^{-x}}{1-R_0^2 e^{-2x}} - \frac{R_0 (1-R_0) e^{-2x}}{1-R_0^2 e^{-2x}} \right\}$$

$$= (1-R_0) \left\{ \frac{1 - (1-R_0) e^{-x} - R_0 e^{-2x}}{1-R_0^2 e^{-2x}} \right\}$$

$$= (1-R_0) \left\{ \frac{1 - (1-R_0)[1 - x + \frac{1}{2}x^2 \dots] - R_0[1 - 2x + 2x^2 \dots]}{1 - R_0^2 e^{-2x}} \right\}$$

$$= (1-R_0) \left\{ \frac{x + R_0 x - \frac{1}{2}x^2 - \frac{3}{2}R_0 x^2}{1 - R_0^2 e^{-2x}} \right\}$$

$$= \frac{x - R_0^2 x - \frac{1}{2}x^2 - R_0 x^2 + \frac{3}{2}R_0^2 x^2}{1 - R_0^2(1-2x + 2x^2)}$$

$$= \frac{1 - R_0^2 - \frac{1}{2}x - R_0 x + \frac{3}{2}R_0^2 x}{1 - R_0^2 + 2R_0^2 x - 2R_0^2 x^2} \cdot x$$

APPENDIX A (cont'd)

$$\lim_{x \ll 1} \left[\frac{1 - R_o^2 - \frac{1}{2}x - R_o x + \frac{3}{2} R_o^2 x}{1 - R_o^2 + 2R_o^2 x - 2R_o^2 x^2} \cdot x \right] = \lim_{x \ll 1} \left[\frac{1 - R_o^2}{1 - R_o^2} \cdot x \right] = x$$

$$\therefore \lim_{\alpha d \ll 1} [1 - T - R] \rightarrow \alpha d$$

APPENDIX B (variation of absorption coefficient with temperature)

(From the paper by H. Nakanishi⁽²⁹⁾).

"The absorption spectra of CdIn₂S₄ have been measured at various temperatures between 4.7 K and 412 K, and analysed in the region of the absorption coefficient from 1 to 2 x 10⁴ cm⁻¹. The data are interpreted as indicating there is direct-allowed transition with an energy gap of 2.75 eV at 0 K. Indirect-allowed transition is also observed with an energy gap of 2.44 eV at 0 K."

Now for indirect-allowed transitions, the absorption coefficient α for a single-phonon process is given by⁽⁴⁰⁾

$$\alpha = \frac{A (h\nu - E_{gi} + E_p)^2}{h\nu [\exp(E_p/kT) - 1]} + \frac{B (h\nu - E_{gi} - E_p)^2}{h\nu [1 - \exp(-E_p/kT)]}$$

where A and B are positive constants which are nearly independent of the photon energy $h\nu$, E_p is the phonon energy, E_{gi} is the indirect energy gap, T is the absolute temperature, and k is the Boltzmann constant. The first term of the equation corresponds to phonon absorption and contributes in the range $h\nu > E_{gi} - E_p$, whereas the second term, the phonon emission term, contributes in the range $h\nu > E_{gi} + E_p$. At very low temperatures, the phonon density is very small, therefore, the first term of the equation is negligible compared with the second. Furthermore, the phonon energy does not change much over the temperature range 100 to 300 K, whereas the energy gap change from 2.45 eV at LNT to 2.28 eV at RT. Neglecting the first term of the equation; one can see that for a fixed photon energy ($h\nu = 2.10$ eV ; $\lambda = 600$ nm), the absorption coefficient should be higher at RT than at LNT because of the decrease of E_{gi} with temperature and because at RT, the contribution of the first term becomes important.

8

8

REFERENCES

1. E. Fortin and F. Raga, Solid State Comm. 14: 847 (1974).
2. E. Grilli, M. Guzzi, A. Anedda, F. Raga and A. Serpi, Solid State Comm. 27: 105 (1978).
3. A. Anedda, L. Cugusi, E. Grilli, M. Guzzi, F. Raga and A. Spiga, Solid State Comm. 29: 829 (1979).
4. L. Krausbauer, R. Nitsche and P. Wild, Proc. Internat. Conf. Luminescence, Budapest (1966).
5. D. Manca, F. Raga and A. Spiga, Nuovo Ciment. 19B: 15 (1974).
6. M. Guzzi and G. Baldini, J. Lum. 9: 514 (1975).
7. A. Serpi, J. Phy. D9: 1881 (1976).
8. A. Anedda, L. Garbato, F. Raga and A. Serpi, Phys. Stat. Sol. (a) 50: 643 (1978).
9. A. Bosacchi, G. Bosacchi, S. Franchi and L. Hernandez, Solid State Comm. 13: 1805 (1973).
10. E. Grilli, M. Guzzi and R. Molteni, Phys. Stat. Sol. (a) 37: 399 (1976).
11. E. Grilli, M. Guzzi, Phys. Stat. Sol. (a) 40: 69 (1977).
12. E. Grilli, P. Cappelletti and M. Guzzi, Phys. Stat. Sol. (a) 50: K93 (1978).
13. E. Grilli, M. Guzzi, P. Cappalletti and A.V. Moshalonov, Phys. Stat. Sol. (a) 59: 755 (1980).
14. E. Grilli and M. Guzzi, Nuovo Cimento 2D: 1927 (1983):

15. W. Czaja and L. Krausbauer, *Phy. Stat. Sol.* 33: 191 (1969).
16. H. Nakanishi, H. Miyashita, S. Endo and T. Irie, *Japan J. Appl. Phys.* 20: 1481 (1981).
17. N.S. Botivents, V.P. Drogyazko and V.K. Niturev, *Soc. Phys. Semicond.* 2: 867 (1969).
18. G.B. Abdullaev, V.B. Antonov, D.T. Guseinov, R.Kh. Nanu and E. Yu. Salaev, *Sov. Phys. Semicond.* 2: 878 (1969).
19. I.A. Damashkin, S.L. Pyshkin, E.I. Radautsan and V.E. Tezlevan, *Optoelectronics* 5: 405 (1973).
20. N.V. Josi, C.E. Rodriguez and A.B. Vincent, *Nuovo Cimento* 2D: 1906 (1983).
21. A.N. Georgobiani, A.N. Gruzintsev, Z.P. Ilyukhina, V.E. Tezlevan and I.M. Tizinanu, *Phys. Stat. Sol. (a)* 82: 207 (1984).
22. S.I. Radautsan, I.P. Molodyan, H.N. Syrbu, V.E. Tezlevan and M.A. Shipitka, *Phys. Stat. Sol. (b)* 49: K175 (1972).
23. Y. Seki, S. Endo and T. Irie, *Japan J. Appl. Phys.* 19: 1667 (1980).
24. H. Nakanishi, S. Endo and T. Irie, *Japan J. Appl. Phys.* 12: 1646 (1973).
25. S.I. Radautsan, N.N. Syrbu, V.E. Tezlevan, K.F. Sherban and N.P. Baran, *Phys. Stat. Sol. (b)* 57: K93 (1973).
26. G.B. Abdullaev, D.A. Guseinova, T.G. Kerimova and R.K.H. Nani, *Soviet Phys. Semicond.* 8: 785 (1974).
27. H. Ihara, H. Abe, S. Endo and T. Irie, *Solid State Comm.* 28: 563 (1978).

28. A. Baldereschi, F. Meloni, F. Aymerich and G. Mula, Inst. Phys. Conf. Ser. 35: 193 (1977).
29. H. Nakanishi, Japan J. Appl. Phys. 19: 103 (1980).
30. W. Czaja, Phys. Kondens. Materie 10: 299 (1970).
31. H. Fujita and Y. Okada, Japan J. Appl. Phys. 13: 1823 (1974).
32. R.H. Bube and C.T. Ho, J. Appl. Phys. 37: 4132 (1966).
33. A. Rose, Concepts in Photoconductivity and Applied Problems (1963).
34. R.H. Bube, Photoconductivity of Solids (1960).
35. S.I. Radautsan, V.P. Gribkovskii, A.E. Tsurkan, L.G. Zimin, V.I. Verln and N.K. Samuilova, Sov. J. Quat. Elect. 6: 1347 (1977).
36. G.A. Abdullaev, G.L. Belenkii, Sov. Phys. Semic. 5: 328 (1971).
37. G.K. Celler, S. Mishra, Appl. Phys. Letters 27: 297 (1975).
38. S. Endo, T. Irie, J. Phys. Chem. Solids 37: 201 (1976).
39. C. Curie; Luminescence crystalline (1960)
40. T.S. Moss, G.J. Burnell and B. Ellis: Semiconductor Opto-Electronics (Butterworths, London) chap. 3.